

Heat Bath Particle Number Spectrum

P.Jizba*

DAMTP, University of Cambridge, Silver Street, Cambridge, CB3 9EW, UK

Abstract

We calculate the number spectrum of particles radiated during a scattering into a heat bath using the thermal largest-time equation and the Dyson-Schwinger equation. We show how one can systematically calculate $\frac{d\langle N(\omega) \rangle}{d\omega}$ to any order using modified real time finite-temperature diagrams. Our approach is demonstrated on a simple model where two scalar particles scatter, within a photon-electron heat bath, into a pair of charged particles and it is shown how to calculate the resulting changes in the number spectra of the photons and electrons.

1 Introduction

In recent years much theoretical effort has been invested in the understanding of relativistic heavy ion collisions as these can create critical energy densities which are large enough to produce the quark-gluon plasma (the deconfined phase of quarks and gluons) [1, 2].

A natural tool for testing the quark-gluon plasma properties would be to look for the particle number spectrum formed when a particle decays within the plasma itself. As the plasma created during heavy ion collisions is, to a very good approximation, in thermodynamical equilibrium [1] (somewhat like a “microwave oven” or a heat bath), one can use the whole machinery of statistical physics and QFT in order to predict the final plasma number spectrum. Such calculations, derived from first principles, were carried out by Landshoff and Taylor [3].

Our aim was to find a sufficiently easy mathematical formalism allowing us to perform mentioned calculations to any order. Because unstable particles treated in [3] can not naturally appear in asymptotic states, we demonstrate our approach on a mathematically more correct (but from practical point of view less relevant) process; namely on the scattering of two particles inside of a heat bath. The method presented here however, might be applied as well to a decay itself (provided that the corresponding decay rate is much less than any of the characteristic energies of the process). In this paper we formulate the basic diagrammatic rules for the methodical perturbative calculus of plasma particle number spectrum $\frac{d\langle N(\omega) \rangle}{d\omega}$ and discuss it in the simple case of a heat bath comprised of photons and electrons, which are for simplicity treated as scalar particles. In Section 2

*E-mail: pj10006@damtp.cam.ac.uk

we review the basic concepts and techniques needed from the theory of the largest-time equation (both for $T = 0$ and $T \neq 0$) and the Dyson- Schwinger equation. Rules for the cut diagrams at finite-temperature are derived and subsequently extended to the case when unheated fields are present. It was already pointed out in ^[4] that the thermal cut diagrams are virtually the Kobes-Semenoff diagrams ^[1] in the Keldysh formalism ^[5]. This observation will allow us to identify type 1 vertices in the real time finite-temperature diagrams with the uncircled vertices used in the (thermal) cut diagrams, and similarly type 2 vertices will be identified with the circled, cut diagram vertices. As we want to restrict our attention to only some particular final particle states, further restrictions on the possible cut diagrams must be included. We shall study these restrictions in the last part of Section 2.

As we shall show in Section 3, the heat-bath particle number spectrum can be conveniently expressed as a fraction. Whilst it is possible to compute the denominator by means of the thermal cut diagrams developed in Section 2, the calculation of the numerator requires more care. Using the Dyson-Schwinger equation, we shall see in Section 4 that it can be calculated through modified thermal cut diagrams. The modification consists of the substitution in turn of each heat bath particle propagator by an altered one. We also show that there must be only one modification per diagram. From this we conclude that from each individual cut diagram we get n modified ones (n stands for the total number of heat-bath particle propagators in the diagram). Furthermore, in the case when more types of the heat bath particles are present, one might be only interested in the number spectrum of some of these. The construction of the modified cut diagrams in such cases follow the same procedure as in the previous situation. We find that only the propagators affiliated to the desired fields must be altered.

In Section 5 the presented approach is applied to a toy model in which the quark-gluon plasma is simulated by *scalar* photons and electrons and we calculate the resulting changes in the number spectrum of the “plasma” particles.

Finally, in Appendix A we derive, directly from the thermal Wick’s theorem, the (thermal) Dyson-Schwinger equation as well as other useful functional identities valid at finite temperature.

2 Basic tools

2.1 Mean statistical value

The central idea of thermal QFT is based on the fact that one can not take the expectation value of an observable A with respect to some pure state as generally all states have non-zero probability to be populated and consequently one must consider instead a mixture of states generally described by the density matrix ρ . The mean statistical value of A is then

$$\langle A \rangle = Tr(\rho A), \tag{2.1}$$

where the trace has to be taken over a complete set of *physical* states. For a statistical system in thermodynamical equilibrium ρ is given by the Gibbs canonical distribution

$$\rho = \frac{e^{-\beta(H-\mu N)}}{\text{Tr}(e^{-\beta(H-\mu N)})} = \frac{e^{-\beta K}}{Z}, \quad (2.2)$$

here Z is the partition function, H is the Hamiltonian, N is the conserved charge (e.g. baryon or lepton number), μ is the chemical potential, $K = H - \mu N$, and β is the inverse temperature: $\beta = 1/T$ ($k_B = 1$).

2.2 Largest-time equation at $T=0$

An important property inherited from zero-temperature QFT is *the largest-time equation* (LTE) [6, 7, 8]. Although the following sections will mainly hinge on the *thermal* LTE, it is instructive to start first with the zero-temperature one. The LTE at $T = 0$ is a generally valid identity which holds for any individual diagram constructed with propagators satisfying certain simple properties. For instance, for the scalar theory one can define the following rules:

$$\begin{aligned} x \text{ --- } 1 \text{ --- } y &\sim i \Delta_F(x-y) \\ x \text{ --- } \underline{2} \text{ --- } y &\sim i \Delta^-(x-y) \\ x \text{ --- } \underline{2} \text{ --- } \underline{1} \text{ --- } y &\sim i \Delta^+(x-y) \\ x \text{ --- } \underline{2} \text{ --- } \underline{2} \text{ --- } y &\sim -i \Delta_F^*(x-y) \end{aligned}$$

The ‘*’ here means complex conjugation. In addition to these rules, each *1st type vertex* has a factor $-ig$ and each *2nd type vertex* has a factor ig . Using this prescription, we can construct diagrams in configuration space. With each diagram then can be associated a function $F(x_1, \dots, x_n)$ having all the 2nd type vertices underlined. For example, for the triangle diagram in Fig.1 we have

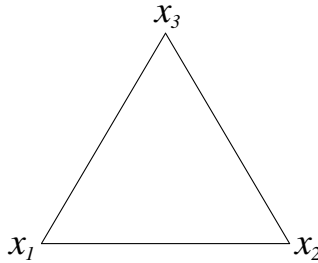


Figure 1: A one loop triangle diagram.

$$\begin{aligned}
F(x_1, x_2, x_3) &= (-ig)^3 i\Delta_F(x_1 - x_2) i\Delta_F(x_1 - x_3) i\Delta_F(x_2 - x_3) \\
F(\underline{x_1}, x_2, x_3) &= (-ig)^2 (ig) i\Delta^+(x_1 - x_2) i\Delta^+(x_1 - x_3) i\Delta_F(x_2 - x_3) \\
F(\underline{x_1}, \underline{x_2}, x_3) &= (ig)^2 (-ig) (-i)\Delta_F^*(x_1 - x_2) i\Delta^+(x_1 - x_3) i\Delta^+(x_2 - x_3) \\
F(\underline{x_1}, \underline{x_2}, \underline{x_3}) &= (ig)^3 (-i)\Delta_F^*(x_1 - x_2) (-i)\Delta_F^*(x_1 - x_3) (-i)\Delta_F^*(x_2 - x_3). \\
&\text{etc.}
\end{aligned}$$

The LTE then states that for a function $F(x_1, \dots, x_n)$ corresponding to some diagram with n vertices

$$F(\dots, \underline{x_i}, \dots) + F(\dots, x_i, \dots) = 0, \quad (2.3)$$

provided that x_{i_0} is the largest time and all other underlinings in F are the same. The proof of Eq.(2.3) is based on an observation that the propagator $i\Delta_F(x)$ can be decomposed into positive and negative energy parts, i.e.

$$i\Delta_F(x) = \theta(x_0) i\Delta^+(x) + \theta(-x_0) i\Delta^-(x), \quad (2.4)$$

$$i\Delta^\pm(x) = \int \frac{d^4k}{(2\pi)^3} e^{-ikx} \theta(\pm k_0) \delta(k^2 - m^2). \quad (2.5)$$

Incidentally, for x_{i_0} being the largest time this directly implies

$$\begin{aligned}
i\Delta_F(x_j - x_i) &= i\Delta^-(x_j - x_i), \\
-i\Delta_F^*(x_i - x_j) &= i\Delta^-(x_i - x_j), \\
i\Delta_F(0) &= -i\Delta_F^*(0).
\end{aligned} \quad (2.6)$$

As $F(\dots, \underline{x_i}, \dots)$ differs from $F(\dots, x_i, \dots)$ only in the propagators directly connected to x_i - which are equal (see Eq.(2.6)) - and in the sign of the x_i vertex, they must mutually cancel.

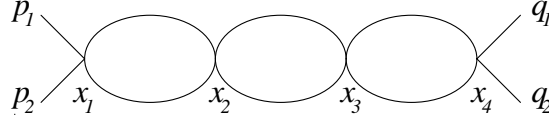
Summing up Eq.(2.3) for all possible underlinings (excluding x_i), we get the LTE where the special rôle of the largest time is not manifest any more, namely

$$\sum_{index} F(x_1, x_2, \dots, x_n) = 0. \quad (2.7)$$

The sum \sum_{index} means summing over all possible distributions of indices 1 and 2 (or equivalently over all possible underlinings). The zero-temperature LTE can be easily reformulated for the T -matrices. Let us remind that the Feynman diagrams for the S -matrix ($S = 1 + iT$) can be obtained by multiplying the corresponding $F(x_1, \dots, x_n)$ with the plane waves for the incoming and outgoing particles, and subsequently integrate over $x_1 \dots x_n$. Thus, in fixed volume quantization a typical n -vertex Feynman diagram is given by

$$\int \prod_{i=1}^n dx_i \prod_j \frac{e^{-ip_j x_{m_j}}}{\sqrt{2\omega_{p_j}} V} \prod_k \frac{e^{iq_k x_{m_k}}}{\sqrt{2\omega_{q_k}} V} F(x_1, \dots, x_n). \quad (2.8)$$

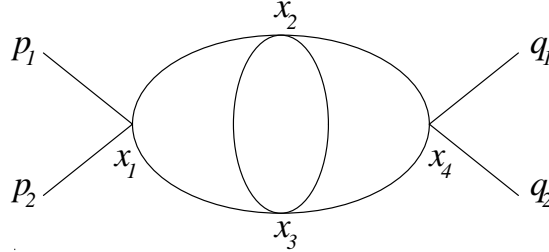
Here the momenta $\{p_j\}$ are attached to incoming particles at the vertices $\{x_{m_j}\}$, while momenta $\{q_k\}$ are attached to outgoing particles at the vertices $\{x_{m_k}\}$. In order to distinguish among various functions $F(x_1, \dots, x_n)$ with the same variables x_1, \dots, x_n , we shall attach a subscript l_n to each function F . For instance, the function $F_{14}(x_1, \dots, x_4)$ corresponding to the diagram



contributes to $\langle q_1 q_2 | iT | p_1 p_2 \rangle$ by

$$\int \prod_{i=1}^4 dx_i \frac{e^{-i(p_1+p_2)x_1}}{V \sqrt{4\omega_{p_1}\omega_{p_2}}} \frac{e^{i(q_1+q_2)x_4}}{V \sqrt{4\omega_{q_1}\omega_{q_2}}} (i\Delta_F(x_1 - x_2))^2 (i\Delta_F(x_2 - x_3))^2 (i\Delta_F(x_3 - x_4))^2,$$

similarly, the function $F_{24}(x_1, \dots, x_4)$ corresponding to the diagram



contributes to $\langle q_1 q_2 | iT | p_1 p_2 \rangle$ by

$$\int \prod_{i=1}^4 dx_i \frac{e^{-i(p_1+p_2)x_1}}{V \sqrt{4\omega_{p_1}\omega_{p_2}}} \frac{e^{i(q_1+q_2)x_4}}{V \sqrt{4\omega_{q_1}\omega_{q_2}}} i\Delta_F(x_1 - x_2) i\Delta_F(x_1 - x_3) (i\Delta_F(x_2 - x_3))^2 \\ \times i\Delta_F(x_4 - x_3) i\Delta_F(x_4 - x_2),$$

etc.

This can be summarized as

$$\langle \{q_k\} | iT | \{p_j\} \rangle = \sum_n \int \dots \int \prod_{i=1}^n dx_i \sum_{l_n} \prod_j \frac{e^{-ip_j x_{m_j}}}{\sqrt{2\omega_{p_j}} V} \prod_k \frac{e^{iq_k x_{m_k}}}{\sqrt{2\omega_{q_k}} V} F_{l_n}(x_1, \dots, x_n), \quad (2.9)$$

Consider now the case $|\{p_j\}\rangle = |\{q_k\}\rangle$ (let us call it $|a\rangle$). From the unitarity condition: $T - T^\dagger = iT^\dagger T$, we get

$$\langle a|T|a\rangle - \langle a|T|a\rangle^* = i\langle a|T^\dagger T|a\rangle. \quad (2.10)$$

On the other hand, by construction $F(\underline{x}_1, \dots, \underline{x}_n) = F^*(x_1, \dots, x_n)$, and thus (see (2.7))

$$F(x_1, \dots, x_n) + F^*(x_1, \dots, x_n) = - \sum_{index'} F(x_1, \dots, x_n). \quad (2.11)$$

The prime over *index* in (2.11) indicates that we sum neither over diagrams with all type 1 vertices nor diagrams with all type 2 vertices. Using (2.9), and identifying $|\{q_k\}\rangle$ with $|\{p_k\}\rangle$ ($= |a\rangle$) we get

$$\langle a|T|a\rangle - \langle a|T|a\rangle^* = - \sum_{index'} \langle a|T|a\rangle, \quad (2.12)$$

or (see (2.10))

$$\langle a|T^\dagger T|a\rangle = i \sum_{index'} \langle a|T|a\rangle. \quad (2.13)$$

Eq.(2.12) is the special case of the LTE for the T -matrices. The finite-temperature extension of (2.13) will prove crucial in Section 4.

Owing to the $\theta(\pm k_0)$ in $\Delta^\pm(x)$ (see Eq.(2.5)), energy is forced to flow only towards type 2 vertices. From both the energy-momentum conservation in each vertex and from the energy flow on the external lines, a sizable class of the diagrams on the RHS's of (2.12)-(2.13) will be automatically zero. Particularly regions of either 1st or 2nd type vertices which are not connected to any external line violate the energy conservation and thus do not contribute (no islands of vertices), see Fig.2. Consequently, the only surviving diagrams are those whose any 1st type vertex area is connected to incoming particles and any 2nd type vertex area is connected to outgoing ones. From historical reasons the border between two regions with different type of vertices is called *cut* and corresponding diagrams are called *cut diagrams*.

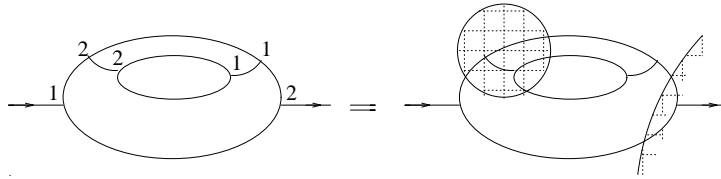


Figure 2: An example of a cut diagram in the φ^3 theory which does not contribute to the RHS's of (2.12)-(2.13). Arrows indicate the flow of energy.

We have just proved a typical feature of $T = 0$ QFT, namely any cut diagram is divided by the cut into two areas only, see Fig.3. Eq.(2.12), rewritten in terms of the cuttings is so called *cutting equation* (or Cutkosky's cutting rules) [6, 7, 8].

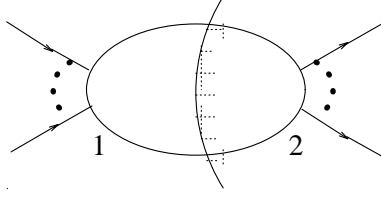


Figure 3: *Generic form of the cut diagram at the $T = 0$. Shadow is on the 2nd type vertex area.*

One point should be added. Inserting the completeness relation $\sum_f |f\rangle\langle f| = 1$ into the LHS of (2.13), we get

$$\sum_f \langle a|T^\dagger|f\rangle\langle f|T|a\rangle = i \sum_{cuts} \langle a|T|a\rangle. \quad (2.14)$$

It may be shown [4, 6] that all the intermediate particles in $|f\rangle$ correspond to cut lines. This has a natural extension when $\langle a|T^\dagger T|a\rangle \rightarrow \langle a|T^\dagger \mathcal{P}T|a\rangle$ with \mathcal{P} being a projection operator ($\mathcal{P} = \mathcal{P}^\dagger = \mathcal{P}^2$) which eliminates some of the states $|f\rangle$. It is easy to see that in such case

$$\langle a|T^\dagger \mathcal{P}T|a\rangle = i \sum_{cuts}^{\sim} \langle a|T|a\rangle, \quad (2.15)$$

where tilde over the \sum_{cuts} indicates that one sums over the diagrams which do not have the cut lines corresponding to particles removed by \mathcal{P} .

There is no difficulty in applying the previous results to spin- $\frac{1}{2}$ [6, 7]. The LTE follows as before: the diagram with only iS_F propagators (and $-ig$ per each vertex) plus the diagram with only $(i\hat{S}_F)$ propagator* (and ig per each vertex) equals to minus the sum of all diagrams with one up to $n - 1$ the type 2 vertices (n being the total number of vertices). For gauge fields more care is needed. Using the Ward identities one can show [6] that type 1 and type 2 vertices in (2.12)-(2.13) may be mutually connected only by *physical particle* propagators (i.e. neither through the propagators corresponding to particles with non-physical polarizations or Fadeev-Popov ghosts and antighosts).

2.3 Thermal Wick's theorem (the Dyson-Schwinger equation)

The key observation at finite temperature is that for systems of *non-interacting* particles in thermodynamical equilibrium Wick's theorem is still valid, i.e. one can decompose the $2n$ -point (free) thermal Green function into a product of two-point (free) thermal Green functions. This may be defined recursively by

The function $i\hat{S}_F(x)$, similarly as $(i\Delta_F)^(x)$, interchanges the rôle S^+ and S^- . Unlike bosons, for fermions $i\hat{S}_F(x)$ is not equal to $(iS_F)^*(x)$. Despite that, Eq.(2.12) still holds [6].

$$\langle \mathcal{T}(\psi(x_1) \dots \psi(x_{2n})) \rangle_\beta = \sum_{\substack{j \\ j \neq i}} \varepsilon_P \langle \mathcal{T}(\psi(x_i) \psi(x_j)) \rangle_\beta \langle \mathcal{T}(\prod_{k \neq i; j} \psi(x_k)) \rangle_\beta, \quad (2.16)$$

where ε_P is the signature of the permutation of fermion operators (= 1 for boson operators) and \mathcal{T} is the standard time ordering symbol. We shall use, from now on, the subscript β , emphasizing that the thermal mean value describes a system in thermodynamical equilibrium (at the temperature β^{-1}). Note that the choice of “ i ” in (2.16) is completely arbitrary. The proof can be found for example in [1, 9, 10]. Similarly as at $T = 0$, Wick’s theorem can also be written for the (free) thermal Wightman functions [9, 14], i.e.

$$\langle \psi(x_1) \dots \psi(x_{2n}) \rangle_\beta = \sum_{\substack{j \\ j \neq 1}} \varepsilon_P \langle \psi(x_1) \psi(x_j) \rangle_\beta \langle \prod_{k \neq 1; j} \psi(x_k) \rangle_\beta. \quad (2.17)$$

A particularly advantageous form of this is the so called Dyson-Schwinger equation (see Appendix A) which, at the $T \neq 0$, reads

$$\langle G[\psi] \psi(x) F[\psi] \rangle_\beta = \int dz \langle \psi(x) \psi(z) \rangle_\beta \left\langle G[\psi] \frac{\vec{\delta} F[\psi]}{\delta \psi(z)} \right\rangle_\beta + \int dz \langle \psi(z) \psi(x) \rangle_\beta \left\langle \frac{G[\psi]}{\delta \psi(z)} \overleftarrow{\delta} F[\psi] \right\rangle_\beta, \quad (2.18)$$

where $\psi(x)$ is an interaction-picture field and $G[\dots]$ and $F[\dots]$ are functionals of ψ . The arrowed variations $\frac{\delta}{\delta \psi(z)}$ are defined as a formal operation satisfying two conditions, namely:

$$\frac{\vec{\delta}}{\delta \psi_n(z)} (\psi_m(x) \psi_q(y)) = \frac{\delta \psi_m(x)}{\delta \psi_n(z)} \psi_q(y) + (-1)^p \psi_m(x) \frac{\delta \psi_q(y)}{\delta \psi_n(z)}, \quad (2.19)$$

or

$$(\psi_m(x) \psi_q(y)) \frac{\overleftarrow{\delta}}{\delta \psi_n(z)} = (-1)^p \frac{\delta \psi_m(x)}{\delta \psi_n(z)} \psi_q(y) + \psi_m(x) \frac{\delta \psi_q(y)}{\delta \psi_n(z)}, \quad (2.20)$$

with

$$\frac{\delta \psi_m(x)}{\delta \psi_n(y)} = \delta(x - y) \delta_{mn}. \quad (2.21)$$

The “ p ” is 0 for bosons and 1 for fermions; subscripts m, n suggest that several types of fields can be generally present. Note, for bosons $\frac{\vec{\delta} F}{\delta \psi} = \frac{F \overleftarrow{\delta}}{\delta \psi}$ which we shall denote as $\frac{\delta F}{\delta \psi}$. For more details see Appendix A.

2.4 Thermal largest-time equation

The LTE (2.13) can be extended to the finite-temperature case, too. Summing up in (2.13) over all the eigenstates of K ($= H - \mu N$) with the weight factor $e^{-\beta K_i}$ (i labels the eigenstates), we get

$$\langle TT^\dagger \rangle_\beta = i \sum_{index'} \langle T \rangle_\beta. \quad (2.22)$$

Let us consider the RHS of (2.22) first. The corresponding thermal LTE and diagrammatic rules (Kobes-Semenoff rules ^[1]) can be derived precisely the same way as at $T = 0$ using the previous, largest-time argumentation ^[1, 16]. It turns out that these rules have basically identical form as those in the previous Section, with an exception that now $\langle 0 | \dots | 0 \rangle \rightarrow \langle \dots \rangle_\beta$. Note that labeling vertices by 1 and 2 we have naturally got a doubling of the number of degrees of freedom. This is a typical feature of the *real-time formalism* in thermal QFT (here, in so called *Keldysh version* ^[1]).

We should also emphasize that it may happen some fields are not thermalized. For example, external particles entering a heat bath or particles describing non-physical degrees of freedom ^[20]. Particularly, if some particles (with momenta $\{p_j\}$) enter the heat bath, the mean statistical value of an observable A is then

$$\begin{aligned} \sum_i \frac{e^{-\beta K_i}}{Z} \langle i; \{p_j\} | A | i; \{p_j\} \rangle &= Z^{-1} \text{Tr}(\rho_{\{p_j\}} \otimes e^{-\beta K} A), \\ \rho_{\{p_j\}} &= |\{p_j\}\rangle \langle \{p_j\}|, \end{aligned}$$

which we shall denote as $\langle A \rangle_{\{p_j\}, \beta}$. From this easily follows the generalization of (2.22)

$$\langle TT^\dagger \rangle_{\{p_k\}, \beta} = i \sum_{index'} \langle T \rangle_{\{p_k\}, \beta}. \quad (2.23)$$

Unlike $T = 0$, we find that the cut diagrams have disconnected vertex areas and no kinematic reasonings used in last Section can, in general, get rid of them. This is because the thermal part of $\langle \varphi(x) \varphi(y) \rangle_\beta$ [†] describes the absorption of on shell particle from the heat bath or the emission of one into it. Thus, at $T \neq 0$, there is no definite direction of transfer of energy from type 1 vertex to type 2 one as energy flows in both directions. Some cut diagrams nevertheless vanish. It is simple to see that only those diagrams survive in which the non-thermalized external particles “enter” a diagram via the 1st type vertices and “leave” it via the 2nd type ones. We might deduce this from the definition of $\langle T \rangle_{\{p_j\}, \beta}$, indeed

$$\sum_{index'} \langle T \rangle_{\{p_j\}, \beta} = \sum_{index'} \sum_i \frac{e^{-\beta K_i}}{Z} \langle i; \{p_j\} | T | i; \{p_j\} \rangle. \quad (2.24)$$

Note, we get the same set of thermal cut diagrams interchanging the summation $\sum_{index'}$ with \sum_i . It is useful to start then with $\sum_{index'} \langle i; \{p_j\} | T | i; \{p_j\} \rangle$. This is, as usual, described by the ($T = 0$) cutting rules. In the last Section we learned that the general structure of the corresponding cut diagrams is depicted in Fig.3, particularly the external particles enter the cut diagram via type 1 vertices and leave it via type 2 ones. Multiplying

[†]Note that $\langle \varphi(x) \varphi(y) \rangle_\beta = \langle : \varphi(x) \varphi(y) : \rangle_\beta + \langle 0 | \varphi(x) \varphi(y) | 0 \rangle$ and $\langle : \varphi(x) \varphi(y) : \rangle_\beta = \int \frac{d^4 k}{(2\pi)^3} f_B(k_0) \delta(k^2 - m^2) e^{-ik(x-y)}$, with $f_B(k_0) = (e^{\beta |k_0|} - 1)^{-1}$.

each diagram (with the external particles in the state $|i; \{p_j\}\rangle$) with the prefactor $\frac{e^{-\beta K_i}}{Z}$ and summing subsequently over i , we again retrieve the thermal cut diagrams, though now it becomes evident that the particles $\{p_j\}$ enter such diagram only via type 1 vertices and move off only through type 2 ones, since the summation of the $(T = 0)$ cut diagrams from which it was derived does not touch lines corresponding to unheated particles. Note, the latter analysis naturally explains why the unheated particles obey the $(T = 0)$ LTE diagrammatic rules even in the thermal diagrams

Another vanishing comes from kinematic reasons. Namely three-leg vertices with all the on shell particles (1-2 lines) can not conserve energy-momentum and consequently the whole cut diagram is zero. As an illustration let us consider all the non-vanishing, topologically equivalent cut diagrams of given type involved in a three-loop contribution to $i \sum_{index'} \langle T \rangle_{pq,\beta}$ (see Fig.4). [‡]

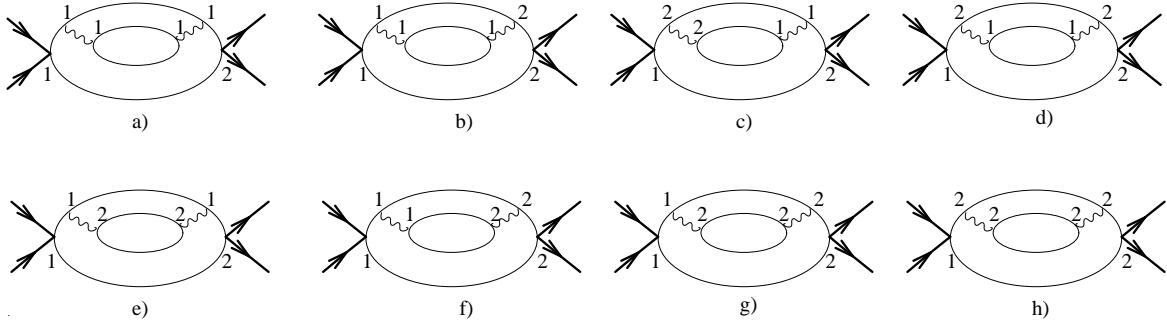


Figure 4: An example of non-vanishing cut diagrams at the $T \neq 0$. The heat-bath consists of two different particles. External particles are not thermalized.

Let us stress one more point. In contrast with $T = 0$, at finite temperature the cut itself neither is unique nor defines topologically equivalent areas, see Fig.5, only the number of crossed legs is, by definition, invariant.

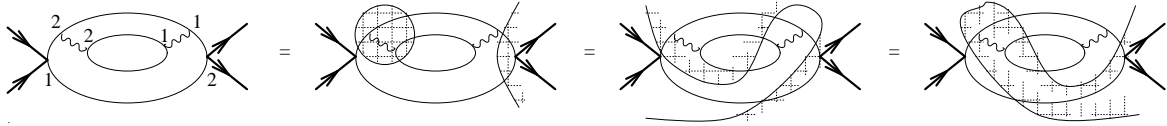


Figure 5: The cut diagram from Fig.3 c) demonstrates that the cut can be defined in many ways but the number of crossed lines is still the same.

This ambiguity shows that the concept of the cut is not very useful at finite temperature and in the following we shall refrain from using it.

In Chapter 4 it will prove useful to have an analogy of (2.23) for $\langle T^\dagger \mathcal{P} T \rangle_\beta$. Here \mathcal{P} is the projection operator defined as

[‡]Let us emphasize that originally we had the 64 possible cut diagrams.

$$\mathcal{P} = \sum_j |a; j\rangle \langle a; j|, \quad (2.25)$$

where “ j ” denotes the physical states for the heat-bath particles and “ a ” labels the physical states for the outgoing, non-thermalized particles. Let us deal with $\langle T^\dagger \mathcal{P} T \rangle_\beta$. Using (2.15), we acquire

$$\langle T^\dagger \mathcal{P} T \rangle_\beta = i \sum_l \frac{e^{-\beta K_l}}{Z} \sum_{index'} \langle l | T | l \rangle. \quad (2.26)$$

Interchanging the summations, we finally arrive at

$$\langle T^\dagger \mathcal{P} T \rangle_\beta = i \sum_{index'} \langle T \rangle_\beta, \quad (2.27)$$

where tilde over the $\sum_{index'}$ means that we are restricted to consider the cut diagrams, with only (1-2)-particle lines corresponding to the “ a ” and “ j ” particles (i.e $\langle 0 | \varphi(x) \varphi(y) | 0 \rangle$ and $\langle \psi(x) \psi(y) \rangle_\beta$, respectively). The extension of Eq.(2.27) to the case where some external, non-thermalized particles $\{p_k\}$ are present is obvious, and reads

$$\langle T^\dagger \mathcal{P} T \rangle_{\{p_k\}, \beta} = i \sum_{index'} \langle T \rangle_{\{p_k\}, \beta}. \quad (2.28)$$

Finally, let us note that using the LTE, one may extend the previous treatment to various Green functions. The LTE for Green’s functions is then a useful starting point for dispersion relations, see e.g. [1, 16].

3 Heat-Bath particle number spectrum: general framework

The cutting equation (2.28) can be fruitfully used for both the partition function Z and the heat-bath particle number spectrum $\frac{d\langle N(\omega) \rangle}{d\omega}$ calculations. To see that, let us for simplicity assume that two particles (say Φ_1, Φ_2) scatter inside a heat bath. We are interested in the heat-bath number spectrum after two different particles (say ϕ_1, ϕ_2) appear in the final state. Except for the condition that the external particles are different from the heat bath ones, no additional assumption about their nature is needed at this stage.

The initial density matrix ρ_i (i.e. the density matrix describing the physical situation before we introduce the particles $\Phi_1(p_1), \Phi_2(p_2)$ into the oven) can be written as

$$\rho_i = Z_i^{-1} \sum_j e^{-\beta K_j} |j; p_1, p_2\rangle \langle j; p_1, p_2|, \quad (3.1)$$

where “ j ” denotes the set of occupation numbers for the heat bath particles. A long time after the scattering the final density matrix ρ_f reads

$$\rho_f = Z_f^{-1} \sum_j e^{-\beta K_j} \mathcal{P} S |j; p_1, p_2\rangle \langle j; p_1, p_2| S^\dagger \mathcal{P}^\dagger, \quad (3.2)$$

here \mathcal{P} is the projection operator projecting out all the non-heat-bath final states except of $\phi_1(q_1), \phi_2(q_2)$ ones. The S -matrix in (3.2) is defined in a standard way: $S = 1 + iT$. The Z_f in (3.2) must be different from Z_i as otherwise ρ_f would not be normalized to unity. In order that ρ_f satisfy the normalization condition $Tr(\rho_f) = 1$, one finds

$$Z_f = \sum_j e^{-\beta K_j} \langle j; p_1, p_2 | S^\dagger \mathcal{P} S | j; p_1, p_2 \rangle = \langle S^\dagger \mathcal{P} S \rangle_{p_1 p_2, \beta} \quad Z_i = \langle T^\dagger \mathcal{P} T \rangle_{p_1 p_2, \beta} \quad Z_i. \quad (3.3)$$

The key point is that we have used in (3.3) the T - matrix because the initial state $|\Phi_1(p_1), \Phi_2(p_2)\rangle$ is, by definition, different from the final one $|\phi(q_1), \phi(q_2)\rangle$ and consequently $\mathcal{P} S$ can be replaced by $i\mathcal{P} T$. This allows us to calculate Z_f using directly the diagrammatic technique outlined in the preceding Section.

From (2.1) and (3.2) one can directly read off that the number spectrum of the heat bath particles is:

$$\begin{aligned} \frac{d\langle N_l(\omega) \rangle_f}{d\omega} &= \int \frac{d^3 \mathbf{k}}{(2\pi)^3} \delta^+(\omega^2 - \mathbf{k}^2 - m_l^2) \sum_f \langle f | a_l^\dagger(\mathbf{k}; \omega) a_l(\mathbf{k}; \omega) \rho_f | f \rangle \\ &= \int \frac{d^3 \mathbf{k}}{(2\pi)^3} \delta^+(\omega^2 - \mathbf{k}^2 - m_l^2) \frac{\langle T^\dagger \mathcal{P} a_l^\dagger(\mathbf{k}; \omega) a_l(\mathbf{k}; \omega) T \rangle_{p_1 p_2, \beta}}{\langle T^\dagger \mathcal{P} T \rangle_{p_1 p_2, \beta}}, \end{aligned} \quad (3.4)$$

and consequently

$$\langle N_l \rangle_f = \int \frac{d^4 k}{(2\pi)^3} \delta^+(k^2 - m_l^2) \frac{\langle T^\dagger \mathcal{P} a_l^\dagger(k) a_l(k) T \rangle_{p_1 p_2, \beta}}{\langle T^\dagger \mathcal{P} T \rangle_{p_1 p_2, \beta}}, \quad (3.5)$$

where we have used the completeness relation for the final states $|f\rangle$ and $[\mathcal{P}; a^\dagger a] = 0$. The subscript “ l ” denotes which type of heat-bath particles we are interested in. In the following the index will be mostly suppressed.

4 Modified cut diagrams

To proceed further with (3.4) and (3.5), we expand the T -matrix in terms of time-ordered interaction-picture fields, i.e.

$$T[\psi] = \sum_n \int dx_1 \dots \int dx_n \alpha_n(x_1 \dots x_n) \mathcal{T}(\psi(x_1) \dots \psi(x_n)). \quad (4.1)$$

Here ψ represents a heat-bath field in the interaction picture. Other fields (i.e. $\bar{\phi}, \phi$ and Φ) are included in the α_n [§]. An extension of (4.1) to the case where different heat-bath fields are present is natural. Employing (4.1) in $\langle T^\dagger \mathcal{P} T \rangle_{p_1 p_2, \beta}$, one can readily see

[§] When Fermi fields are involved, we have, for the sake of compactness, included in the argument of ψ the space-time coordinate, the Dirac index, and a discrete index which distinguishes ψ_α from $\bar{\psi}_\alpha$.

that this factorizes out in each term of the expansion a *pure* thermal mean value $\langle \dots \rangle_\beta$. The general structure of each such thermal mean value is: $\langle G_m[\psi] F_n[\psi] \rangle_\beta$, where $F_n[\dots]$ and $G_m[\dots]$ are the operators with “ n ” chronological and “ m ” anti-chronological time ordered (heat-bath) fields, respectively. Analogous factorization is true in the expansion of $\langle T^\dagger \mathcal{P} a_l^\dagger a_l \mathcal{P} T \rangle_{p_1 p_2, \beta}$. The only difference is that the pure thermal mean value has the form $\langle G_m[\psi] a^\dagger a F_n[\psi] \rangle_\beta$ instead [¶]. In case when various heat-bath fields are present, $m = m_1 + m_2 + \dots + m_n$, with “ m_l ” denoting the number of the heat-bath fields of l -th type.

Applying the Dyson-Schwinger equation to $\langle G_m[\psi] a^\dagger a F_n[\psi] \rangle_\beta$ twice and summing over “ n ” and “ m ”, we get cheaply the following expression (c.f. also (A.11))

$$\begin{aligned}
\langle T^\dagger \mathcal{P} a_l^\dagger a_l T \rangle_{p_1 p_2, \beta} &= \\
&= \int dx dy \{ \langle \psi_l(x) a_l^\dagger \rangle_\beta \langle a_l \psi_l(y) \rangle_\beta + (-1)^p \langle \psi_l(x) a_l \rangle_\beta \langle a_l^\dagger \psi_l(y) \rangle_\beta \} \left\langle \frac{T^\dagger \overleftarrow{\delta}}{\delta \psi_l(x)} \mathcal{P} \frac{\overrightarrow{\delta} T}{\delta \psi_l(y)} \right\rangle_{p_1 p_2, \beta} \\
&+ \int \frac{dx dy}{2} \{ \langle \psi_l(x) a_l \rangle_\beta \langle \psi_l(y) a_l^\dagger \rangle_\beta + (-1)^p \langle \psi_l(x) a_l^\dagger \rangle_\beta \langle \psi_l(y) a_l \rangle_\beta \} \left\langle \frac{T^\dagger \overleftarrow{\delta^2}}{\delta \psi_l(y) \delta \psi_l(x)} \mathcal{P} T \right\rangle_{p_1 p_2, \beta} \\
&+ \int \frac{dx dy}{2} \{ \langle a_l \psi_l(x) \rangle_\beta \langle a_l^\dagger \psi_l(y) \rangle_\beta + (-1)^p \langle a_l^\dagger \psi_l(x) \rangle_\beta \langle a_l \psi_l(y) \rangle_\beta \} \left\langle T^\dagger \mathcal{P} \frac{\overrightarrow{\delta^2} T}{\delta \psi_l(y) \delta \psi_l(x)} \right\rangle_{p_1 p_2, \beta} \\
&+ \langle a_l^\dagger a_l \rangle_\beta \langle T^\dagger \mathcal{P} T \rangle_{p_1 p_2, \beta}, \tag{4.2}
\end{aligned}$$

A similar decomposition for $\langle T^\dagger \mathcal{P} T \rangle_{p_1 p_2, \beta}$ would not be very useful (cf. (A.18)); instead we define $\langle (T^\dagger \mathcal{P} T)' \rangle_{p_1 p_2, \beta}$ having the same expansion as $\langle T^\dagger \mathcal{P} T \rangle_{p_1 p_2, \beta}$ except for the $\alpha_n(\dots) \mathcal{P} \alpha_m^\dagger(\dots)$ are replaced by $\alpha_n(\dots) \mathcal{P} \alpha_m^\dagger(\dots) \frac{n_l + m_l}{2}$. In this formalism $\langle (T^\dagger \mathcal{P} T)' \rangle_{p_1 p_2, \beta}$ is

$$\begin{aligned}
\langle (T^\dagger \mathcal{P} T)' \rangle_{p_1 p_2, \beta} &= \\
&= \int dx dy \langle \psi_l(x) \psi_l(y) \rangle_\beta \left\langle \frac{T^\dagger \overleftarrow{\delta}}{\delta \psi_l(x)} \mathcal{P} \frac{\overrightarrow{\delta} T}{\delta \psi_l(y)} \right\rangle_{p_1 p_2, \beta} \\
&+ \int \frac{dx dy}{2} \langle \overline{\mathcal{T}}(\psi_l(x) \psi_l(y)) \rangle_\beta \left\langle \frac{T^\dagger \overleftarrow{\delta^2}}{\delta \psi_l(y) \delta \psi_l(x)} \mathcal{P} T \right\rangle_{p_1 p_2, \beta} \\
&+ \int \frac{dx dy}{2} \langle \mathcal{T}(\psi_l(x) \psi_l(y)) \rangle_\beta \left\langle T^\dagger \mathcal{P} \frac{\overrightarrow{\delta^2} T}{\delta \psi_l(y) \delta \psi_l(x)} \right\rangle_{p_1 p_2, \beta}, \tag{4.3}
\end{aligned}$$

with the $\overline{\mathcal{T}}$ being the anti-chronological ordering symbol. Comparing (4.3) with (A.19), we can interpret the RHS of (4.3) as a sum over *all* possible distributions of one line (corresponding to ψ_l) inside of each given ($T \neq 0$!) cut diagram constructed out of

[¶]Remember that $\mathcal{P} = \mathcal{P}' \otimes \mathcal{P}'' = |q_1, q_2\rangle \langle q_1, q_2| \otimes \sum_j |j\rangle \langle j|$. Here $\mathcal{P}'' = \sum_j |j\rangle \langle j|$ behaves as an identity in the subspace of heat-bath states.

$\langle T^\dagger \mathcal{P} T \rangle_{p_1 p_2, \beta}$. As (4.3) has precisely the same diagrammatical structure as $\langle T^\dagger \mathcal{P} a^\dagger a T \rangle_{p_1 p_2, \beta} - \langle a^\dagger a \rangle_\beta \langle T^\dagger \mathcal{P} T \rangle_{p_1 p_2, \beta}$ (cf.(4.2)), it shows that in order to compute the numerator of $\frac{d\Delta\langle N(\omega) \rangle}{d\omega} = \frac{d\langle N(\omega) \rangle_f}{d\omega} - \frac{d\langle N(\omega) \rangle_i}{d\omega}$ || one can simply modify the usual $\langle T^\dagger \mathcal{P} T \rangle_{p_1 p_2, \beta}$ cut diagrams by the following one-line replacements (cf.(3.4)).

(i) For neutral scalar bosons:

$$\begin{aligned}
\langle \varphi(x) \varphi(y) \rangle_\beta &\rightarrow \int \frac{d^3 \mathbf{k}}{(2\pi)^3} \delta^+(\omega^2 - \mathbf{k}^2 - m^2) \{ \langle \varphi(x) a^\dagger(\mathbf{k}; \omega) \rangle_\beta \langle a(\mathbf{k}; \omega) \varphi(y) \rangle_\beta \\
&\quad + \langle \varphi(x) a(\mathbf{k}; \omega) \rangle_\beta \langle a^\dagger(\mathbf{k}; \omega) \varphi(y) \rangle_\beta \} \\
&= \int \frac{d^4 k}{(2\pi)^3} \delta(k^2 - m^2) \{ f_B(\omega) (f_B(\omega) + 1) \\
&\quad \times (\delta^-(k_0 + \omega) + \delta^+(k_0 - \omega)) \\
&\quad + \delta^+(k_0 - \omega) (1 + f_B(\omega)) - \delta^-(k_0 + \omega) f_B(\omega) \} e^{-ik(x-y)}, \quad (4.4)
\end{aligned}$$

where $f_B(\omega)$ is the Bose-Einstein distribution: $f_B(\omega) = \frac{1}{e^{\beta|\omega|} - 1}$. Term $\theta(-k_0) f_B(\omega)$ describes the absorption of a heat-bath particle, so reduces the number spectrum, that is why the negative sign appears in front of it. Analogously,

$$\begin{aligned}
\langle \mathcal{T}(\varphi(x) \varphi(y)) \rangle_\beta &\rightarrow \int \frac{d^3 \mathbf{k}}{(2\pi)^3} \delta^+(\omega^2 - \mathbf{k}^2 - m^2) \{ \langle a^\dagger(\mathbf{k}; \omega) \varphi(x) \rangle_\beta \langle a(\mathbf{k}; \omega) \varphi(y) \rangle_\beta \\
&\quad + \langle a(\mathbf{k}; \omega) \varphi(x) \rangle_\beta \langle a^\dagger(\mathbf{k}; \omega) \varphi(y) \rangle_\beta \} \\
&= \int \frac{d^4 k}{(2\pi)^3} \delta(k^2 - m^2) (1 + f_B(\omega)) f_B(\omega) e^{-ik(x-y)} \\
&\quad \times (\delta^+(k_0 - \omega) + \delta^-(k_0 + \omega)). \quad (4.5)
\end{aligned}$$

Similarly, for $\Delta\langle N \rangle$ one needs the following replacements (cf.(3.5))

$$\begin{aligned}
\langle \varphi(x) \varphi(y) \rangle_\beta &\rightarrow \int \frac{d^4 k}{(2\pi)^3} \delta(k^2 - m^2) \{ f_B(\omega_k) (f_B(\omega_k) + 1) \\
&\quad + \theta(k_0) (1 + f_B(\omega_k)) - \theta(-k_0) f_B(\omega_k) \} e^{-ik(x-y)}, \\
\langle \mathcal{T}(\varphi(x) \varphi(y)) \rangle_\beta &\rightarrow \int \frac{d^4 k}{(2\pi)^3} \delta(k^2 - m^2) (1 + f_B(\omega_k)) f_B(\omega_k) e^{-ik(x-y)}, \quad (4.6)
\end{aligned}$$

with $\omega_k = \sqrt{\mathbf{k}^2 + m^2}$.

|| Here $\frac{d\langle N(\omega) \rangle_i}{d\omega} = \int \frac{d^3 \mathbf{k}}{(2\pi)^3} \delta^+(\omega^2 - \mathbf{k}^2 - m^2) \langle a^\dagger(\omega, \mathbf{k}) a(\omega, \mathbf{k}) \rangle_\beta$, (cf. (3.4)).

(ii) For Dirac fermions:

The Dirac field is comprised of two different types of excitations (mutually connected via charge conjugation), so the corresponding number operator $N(\omega) = N_b(\omega) + N_d(\omega)$ with

$$\begin{aligned} N_b(\omega) &= \sum_{\alpha=1,2} \int \frac{d^3\mathbf{k}}{(2\pi)^3} \delta^+(\omega^2 - \mathbf{k}^2 - m^2) b_\alpha^\dagger(\mathbf{k}; \omega) b_\alpha(\mathbf{k}; \omega) \\ N_d(\omega) &= \sum_{\alpha=1,2} \int \frac{d^3\mathbf{k}}{(2\pi)^3} \delta^+(\omega^2 - \mathbf{k}^2 - m^2) d_\alpha^\dagger(\mathbf{k}; \omega) d_\alpha(\mathbf{k}; \omega). \end{aligned}$$

Thus, the one-line replacements needed for $\frac{d\Delta\langle N_b(\omega) \rangle}{d\omega}$ are

$$\begin{aligned} \langle \psi_\rho(x) \bar{\psi}_\sigma(y) \rangle_\beta &\rightarrow \sum_{\alpha=1,2} \int \frac{d^3\mathbf{k}}{(2\pi)^3} \delta^+(\omega^2 - \mathbf{k}^2 - m^2) \{ \langle \psi_\rho(x) b_\alpha^\dagger(\mathbf{k}; \omega) \rangle_\beta \langle b_\alpha(\mathbf{k}; \omega) \bar{\psi}_\sigma(y) \rangle_\beta \\ &\quad - \langle \psi_\rho(x) b_\alpha(\mathbf{k}; \omega) \rangle_\beta \langle b_\alpha^\dagger(\mathbf{k}; \omega) \bar{\psi}_\sigma(y) \rangle_\beta \} \\ &= \int \frac{d^4k}{(2\pi)^3} \delta^+(k^2 - m^2) \delta(k_0 - \omega) (\not{k} + m)_{\rho\sigma} \\ &\quad \times \{ (1 - f_F(\omega)) - f_F(\omega)(1 - f_F(\omega)) \} e^{-ik(x-y)}, \end{aligned} \tag{4.7}$$

where $f_F(\omega)$ is the Fermi-Dirac distribution: $f_F(\omega) = \frac{1}{e^{\beta(|\omega| - \mu)} + 1}$, and

$$\begin{aligned} \langle \mathcal{T}(\psi_\rho(x) \bar{\psi}_\sigma(y)) \rangle_\beta &\rightarrow \sum_{\alpha=1,2} \int \frac{d^3\mathbf{k}}{(2\pi)^3} \delta^+(\omega^2 - \mathbf{k}^2 - m^2) \{ \langle b_\alpha(\mathbf{k}; \omega) \psi_\rho(x) \rangle_\beta \langle b_\alpha^\dagger(\mathbf{k}; \omega) \bar{\psi}_\sigma(y) \rangle_\beta \\ &\quad - \langle b_\alpha^\dagger(\mathbf{k}; \omega) \psi_\rho(x) \rangle_\beta \langle b_\alpha(\mathbf{k}; \omega) \bar{\psi}_\sigma(y) \rangle_\beta \} \\ &= - \int \frac{d^4k}{(2\pi)^3} \delta^+(k^2 - m^2) \delta(k_0 - \omega) (\not{k} + m)_{\rho\sigma} \\ &\quad \times f_F(\omega)(1 - f_F(\omega)) e^{-ik(x-y)}. \end{aligned} \tag{4.8}$$

Correspondingly, for $\Delta\langle N_b \rangle$ we need

$$\begin{aligned} \langle \psi_\rho(x) \bar{\psi}_\sigma(y) \rangle_\beta &\rightarrow \int \frac{d^4k}{(2\pi)^3} \delta^+(k^2 - m^2) (\not{k} + m)_{\rho\sigma} \\ &\quad \times \{ (1 - f_F(\omega)) - f_F(\omega)(1 - f_F(\omega)) \} e^{-ik(x-y)} \\ \langle \mathcal{T}(\psi_\rho(x) \bar{\psi}_\sigma(y)) \rangle_\beta &\rightarrow - \int \frac{d^4k}{(2\pi)^3} \delta^+(k^2 - m^2) (\not{k} + m)_{\rho\sigma} f_F(\omega)(1 - f_F(\omega)) e^{-ik(x-y)}. \end{aligned} \tag{4.9}$$

For the d -type excitations the prescription is very similar, actually, in order to get $\frac{d\Delta\langle N_d(\omega)\rangle}{d\omega}$, the following substitutions must be performed in (4.7)-(4.9): $\theta(k_0) \rightarrow \theta(-k_0)$, $f_F \rightarrow (1 - f_F)$ and $\mu \rightarrow -\mu$.

(iii) For gauge fields in the axial temporal gauge ($A^0 = 0$):

The temporal gauge is generally incorporated in the gauge fixing sector of the Lagrangian and particularly

$$\mathcal{L}_{fix} = -\frac{1}{2\alpha}(A_0)^2; \alpha \rightarrow 0. \quad (4.10)$$

The principal advantage of the axial gauges arises from the decoupling the F-P ghosts in the theory. This statement is of course trivial in QED as any linear gauge (both for covariant and noncovariant case) brings this decoupling automatically ^[1]. Particular advantage of the temporal gauge comes from an elimination of non-physical scalar photons from the very beginning.

Let us decompose a gauge field $A_i, i = 1, 2, 3$ into the transverse and longitudinal part, i.e. $A_i = A_i^T + A_i^L$ with

$$A_i^T = \left(\delta_{ij} - \frac{\partial_i \partial_j}{\bar{\partial}^2} \right) A_j \quad \text{and} \quad A_i^L = \frac{\partial_i \partial_j}{\bar{\partial}^2} A_j, \quad (4.11)$$

and use the sum over gauge-particle polarizations

$$\sum_{\lambda=1}^2 \varepsilon_i^{(\lambda)}(k) \varepsilon_j^{(\lambda)}(k) = \delta_{ij} - \frac{k_i k_j}{\mathbf{k}^2}, \quad (4.12)$$

with $\varepsilon^{(\lambda)}(k)$ being polarization vectors, then for $\frac{d\Delta\langle N^T(\omega)\rangle}{d\omega}$ we get the following one-line replacements

$$\begin{aligned} \langle A_i^T(x) A_j^T(y) \rangle_\beta &\rightarrow \sum_{\lambda=1}^2 \int \frac{d^3 \mathbf{k}}{(2\pi)^3} \delta^+(\omega^2 - \mathbf{k}^2 - m^2) \langle A_i^T(x) a_\lambda^\dagger(\mathbf{k}; \omega) \rangle_\beta \langle a_\lambda(\mathbf{k}; \omega) A_j^T(y) \rangle_\beta \\ &\quad + \langle A_i^T(x) a_\lambda(\mathbf{k}; \omega) \rangle_\beta \langle a_\lambda^\dagger(\mathbf{k}; \omega) A_j^T(y) \rangle_\beta \} \\ &= \left(\delta_{ij} - \frac{\partial_i \partial_j}{\bar{\partial}^2} \right) (\text{Eq. (4.4)}) \\ \langle \mathcal{T}(A_i^T(x) A_j^T(y)) \rangle_\beta &\rightarrow \sum_{\lambda=1}^2 \int \frac{d^3 \mathbf{k}}{(2\pi)^3} \delta^+(\omega^2 - \mathbf{k}^2 - m^2) \{ \langle A_i^T(x) a_\lambda^\dagger(\mathbf{k}; \omega) \rangle_\beta \langle A_j^T(y) a_\lambda(\mathbf{k}; \omega) \rangle_\beta \\ &\quad + \langle A_i^T(x) a_\lambda(\mathbf{k}; \omega) \rangle_\beta \langle A_j^T(y) a_\lambda^\dagger(\mathbf{k}; \omega) \rangle_\beta \} \\ &= \left(\delta_{ij} - \frac{\partial_i \partial_j}{\bar{\partial}^2} \right) (\text{Eq. (4.5)}). \end{aligned} \quad (4.13)$$

The replacements needed for $\Delta\langle N^T \rangle$ can be concisely expressed as

$$\langle \dots \rangle_\beta \rightarrow \left(\delta_{ij} - \frac{\partial_i \partial_j}{\partial^2} \right) \text{ (Eq.(4.6))} \quad (4.14)$$

As for the longitudinal (non-physical) degrees of freedom, it is obvious that

$$\langle A_i^L(x) A_j^L(y) \rangle_\beta; \quad \langle \mathcal{T}(A_i^L(x) A_j^L(y)) \rangle_\beta \rightarrow 0. \quad (4.15)$$

Eqs.(4.4)-(4.14) can be most easily derived in the finite volume limit, e.g. for a scalar field we reformulate $\varphi(x)$ as

$$\varphi(x) = \sum_r \frac{A_r}{\sqrt{2E_r V}} e^{-iE_r t + i\mathbf{k}_r \cdot \mathbf{x}} + \frac{A_r^\dagger}{\sqrt{2E_r V}} e^{iE_r t - i\mathbf{k}_r \cdot \mathbf{x}}, \quad (4.16)$$

rescaling the annihilation and creation operators by defining $a(k) = \sqrt{2E_k V} A_k$ in such a way that $[A_k; A_{k'}^\dagger] = \delta_{kk'}$ (so that $\langle A_k^\dagger A_{k'} \rangle_\beta = \delta_{kk'} f_B(k_0)$), while $\int \frac{d^3 \mathbf{k}}{(2\pi)^3} \rightarrow \frac{1}{V} \sum_{\mathbf{k}}$.

The replacements (4.4)-(4.14) are meant in the following sense: firstly one constructs all the $T \neq 0$ diagrams for $\langle T^\dagger \mathcal{P} T \rangle_{p_1 p_2, \beta}$, using the LTE (2.28) and the rules mentioned therein. In order to calculate the numerator of (3.4) or (3.5) we simply replace (using corresponding prescriptions) *one* heat bath particle line in each cut diagram and this replacement must sum for all the possible heat-bath particle lines in the diagram. If more types of heat-bath particles are present, we replace only those lines which correspond to particles whose number spectrum we want to compute (see Fig.6).

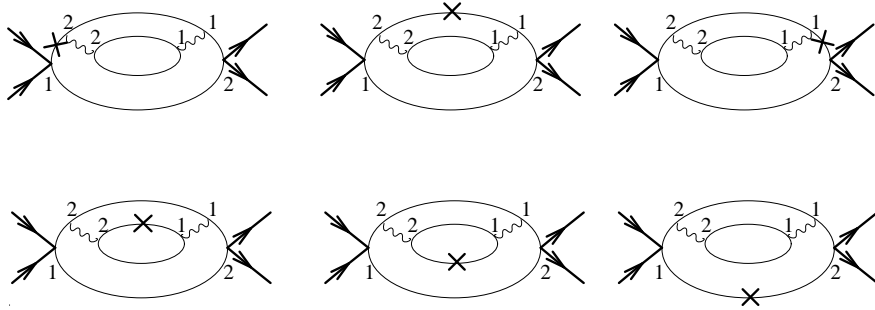


Figure 6: The numerator of (3.4) and (3.5) can be calculated using the modified cut diagrams for $\langle T^\dagger \mathcal{P} T \rangle_{p_1 p_2, \beta}$. As an example we depict all the possible contributions to the numerator derived from the cut diagram on Fig.4 c). The wavy lines and thin lines describe the heat-bath particles. The crossed lines denote the substituted propagators, in this case we wish to calculate the thin-line particle number spectrum.

The terms in the replacements (4.4)-(4.14) have a direct physical interpretation. The $f(\omega_k)$ and $(1 + (-1)^p f(\omega_k))$ can be viewed as the absorption and emission of the heat-bath particles respectively [3]. The term $f(\omega_k)(1 + (-1)^p f(\omega_k))$ describes the fluctuations

of the heat bath particles. This is because for the non-interacting heat-bath particles $\langle (n_k - \langle n_k \rangle_\beta)^2 \rangle_\beta = f(\omega_k)(1 + (-1)^p f(\omega_k))$. The substituted propagators can be therefore schematically depicted as

$$\begin{aligned}
x \text{---} \text{X} \text{---} y &\approx \text{fluctuations} \\
x \text{---} \text{X} \text{---} y &\approx \text{fluctuations} + \text{emissions} + \text{absorptions} \\
x \text{---} \text{X} \text{---} y &\approx \text{fluctuations}
\end{aligned}$$

Collecting all the contributions from emissions, absorptions and fluctuations separately, one can schematically write

$$\frac{d\langle N(\omega) \rangle_f}{d\omega} = \frac{d\langle N(\omega) \rangle_i}{d\omega} + F^{emission}(\omega) + F^{absorption}(\omega) + F^{fluc}(\omega), \quad (4.17)$$

where, for instance for neutral scalar bosons

$$F^{emission}(\omega) = Z_f^{-1} \int \frac{d^4 k}{(2\pi)^3} \delta^+(k^2 - m^2) \delta(k_0 - \omega) (1 + f_B(\omega)) \left\langle \frac{T^\dagger \overleftarrow{\delta}}{\delta\psi(x)} \mathcal{P} \frac{\overrightarrow{\delta} T}{\delta\psi(y)} \right\rangle_{p_1 p_2, \beta}.$$

Using (4.5), it is easy to write down the analogous expressions for the $F^{absorption}$ and F^{fluc} . To the lowest perturbative order, the form (4.17) was obtained by Landshoff and Taylor [3].

5 Model process

5.1 Basic assumptions

To illustrate the modified cut diagram technique, we shall restrict ourselves to a toy model, namely to a scattering of two neutral scalar particles Φ within a photon-electron heat bath, with a pair of scalar charged particles $\phi, \bar{\phi}$ left as a final product. Both initial and final particles are supposed to be unheated. We further assume that the heat bath photons A and electrons Ψ are scalars, i.e. the heat-bath Hamiltonian has form

$$\begin{aligned}
H^{hb} &= H^\gamma + H^e + eA\Psi\Psi^\dagger + \frac{e^2}{2}A^2\Psi\Psi^\dagger \\
H^e &= \partial_\nu\Psi\partial^\nu\Psi^\dagger - m_e^2\Psi\Psi^\dagger \\
H^\gamma &= \frac{1}{2}(\partial_\nu A)^2 - \frac{m_\gamma^2}{2}A^2.
\end{aligned} \quad (5.1)$$

On the other hand H_{in} entering in the T -matrix reads $H_{in} = \frac{\lambda}{2}\Phi^2\phi\phi^\dagger + (eA + \frac{e^2}{2}A^2)\Psi\Psi^\dagger + (eA + \frac{e^2}{2}A^2)\phi\phi^\dagger$. It is usually argued [11, 12] that the interacting pieces in H^{hb} can be dropped provided that $t_i \rightarrow -\infty$ and $t_f \rightarrow \infty$. In the following we accept this omission as it allows us to use safely Wick's theorem (2.16) and Dyson-Schwinger equation (2.18).

5.2 Calculations

We can now compute an order- e^2 contribution to the $\frac{d\Delta\langle N_\gamma(\omega)\rangle}{d\omega}$. The evaluation of the $\frac{d\Delta\langle N_\gamma(\omega)\rangle}{d\omega}$ is straightforward. In Fig.7 we list all the modified cut diagrams contributing to an order- e^2 .

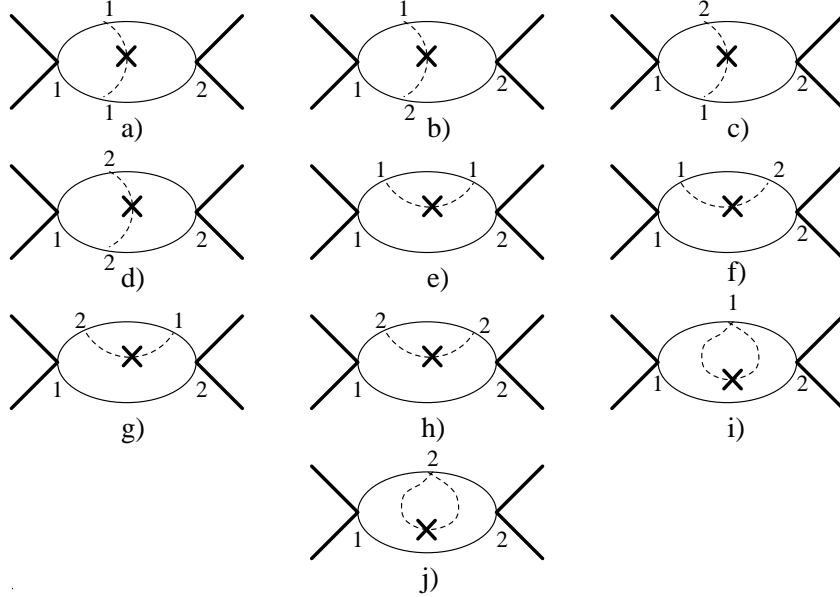


Figure 7: *The modified cut diagrams involved in an order- e^2 contribution to the photon number spectrum. Dashed lines: photons. Solid lines: ϕ , ϕ^\dagger particles. Bold lines: Φ particles.*

Note that diagrams b) and c) are topologically identical. Similarly, diagrams e), f), h), i) and j) should be taken with combinatorial factor 2 (corresponding diagrams for insertion of a heat-bath particle line in the bottom, solid line are omitted). Of course, diagram g) vanishes for kinematic reasons. Let us emphasize that it is necessary to give sense to graphs e), h), i) and j) as these suffer with the pinch singularity; the muon-particle propagator $(p_{1;2}^2 - m^2)^{-1}$ has to be evaluated at its pole because of the presence of an on-shell line (1-2 line) with the same momenta. Some regularization is obviously necessary. Using the formal identity ^[1]

$$\frac{1}{x + i\varepsilon}\delta(x) = -\frac{1}{2}\delta'(x) - i\pi(\delta(x))^2, \quad (5.2)$$

we discover that the unwanted δ^2 mutually cancel between e) and h) diagrams (similarly for i) and j) diagrams). An alternative (but lengthier) way of dealing with the latter pinch singularity; i.e. switching off the interaction with a heat bath in the remote past and future, is discussed in ^[18]. Using the prescriptions (4.4)-(4.5) and evaluating the integrals (note, we should attach to each digram the factor $\frac{1}{2!}$ coming from a Taylor expansion of the T -matrix), we are left with (c.f. Eq.(4.17)):

$$\begin{aligned}
& F^{emission}(\omega) + F^{absorption}(\omega) \\
&= \frac{t\lambda^2 e^2}{\langle T\mathcal{P}T^\dagger \rangle_{p_1 p_2, \beta} V 8\omega_{p_1} \omega_{p_2} (2\pi)^5} \int d^4 k \delta(k^2 - m_\gamma^2) \delta(k_0 - \omega) \\
&\quad \times \int d^4 q_1 d^4 q_2 \delta^+(q_1^2 - m_\mu^2) \delta^+(q_2^2 - m_\mu^2) \\
&\quad \times \left\{ K_1 (1 + f(\omega)) \delta^4(-Q + q_1 + q_2 + k) \right. \\
&\quad \left. - K_2 f_B(\omega) \delta^4(-Q + q_1 + q_2 - k) \right\}
\end{aligned} \tag{5.3}$$

and

$$\begin{aligned}
F^{fluct}(\omega) &= \frac{t\lambda^2 e^2 f_B(\omega) (1 + f_B(\omega))}{\langle T\mathcal{P}T^\dagger \rangle_{p_1 p_2, \beta} V 8\omega_{p_1} \omega_{p_2} (2\pi)^5} \int d^4 k \delta(k^2 - m_\gamma^2) \delta(k_0 - \omega) \\
&\quad \times \int d^4 q_1 d^4 q_2 \delta^+(q_1^2 - m_\mu^2) \delta^+(q_2^2 - m_\mu^2) \\
&\quad \times \left\{ \delta^4(-Q + q_1 + q_2 + k) K_1 + \delta^4(-Q + q_1 + q_2 - k) K_2 \right. \\
&\quad \left. - 2\delta^4(-Q + q_1 + q_2) K_3 \right\} \\
&+ \frac{t\lambda^2 e^2 f_B(\omega) (1 + f_B(\omega))}{\langle T\mathcal{P}T^\dagger \rangle_{p_1 p_2, \beta} V 8\omega_{p_1} \omega_{p_2} (2\pi)^5} \int d^4 k \delta(k^2 - m_\gamma^2) \delta(k_0 - \omega) \\
&\quad \times \int d^4 q_1 d^4 q_2 \delta^4(-Q + q_1 + q_2) \\
&\quad \times \left\{ \left(1 - \frac{1}{2q_1 k - m_\gamma^2} + \frac{1}{2q_1 k + m_\gamma^2} \right) \delta^+(q_2^2 - m_\mu^2) \frac{\partial}{\partial m_\mu^2} \delta^+(q_1^2 - m_\mu^2) \right. \\
&\quad \left. + (q_1 \leftrightarrow q_2) \right\}
\end{aligned} \tag{5.4}$$

with $K_1 = \left(\frac{1}{2q_1 k + m_\gamma^2} + \frac{1}{2q_2 k + m_\gamma^2} \right)^2$, $K_2 = \left(\frac{1}{2q_1 k - m_\gamma^2} + \frac{1}{2q_2 k - m_\gamma^2} \right)^2$, $K_3 = \frac{2}{(2q_1 k - m_\gamma^2)(2q_2 k + m_\gamma^2)}$ and $Q = p_1 + p_2$. We have dropped the $i\varepsilon$ prescription in the propagators since adding/subtracting an on-shell momenta $q_{1,2}$ to/from an on-shell momenta k we can not fulfil the condition $(k \pm q_{1,2})^2 = m_\mu^2$. As it is usual, we have assumed that our interaction is enclosed in a ‘time’ and volume box (t and V respectively). The relevant (i.e. order- e^0) term for $\langle T\mathcal{P}T^\dagger \rangle_{p_1 p_2, \beta}$ reads

$$\begin{aligned}
\langle T\mathcal{P}T^\dagger \rangle_{p_1 p_2, \beta} &= \frac{\lambda^2 t}{8V \omega_{p_1} \omega_{p_2} (2\pi)^2} \int d^4 q_1 d^4 q_2 \delta^+(q_1^2 - m_\mu^2) \delta^+(q_2^2 - m_\mu^2) \delta^4(-Q + q_1 + q_2) \\
&= \frac{\lambda^2 t}{64V \omega_{p_1} \omega_{p_2} |Q| \pi} \sqrt{Q^2 - 4m_\mu^2},
\end{aligned} \tag{5.5}$$

Eqs.(5.3) and (5.4) are analogous to the result obtained in [3] for the decay.

One can perform the similar calculations for the electron number spectrum $\frac{d\Delta\langle N_e(\omega)\rangle}{d\omega}$. The task is now, however, tougher. The major difference in comparison with the photon number spectrum is that the lowest order in e (keeping λ^2) is e^4 . This brings richer diagrammatic structure then in the photon case. In Fig.8 we list all the generating thermal diagrams contributing to an order- e^4 .

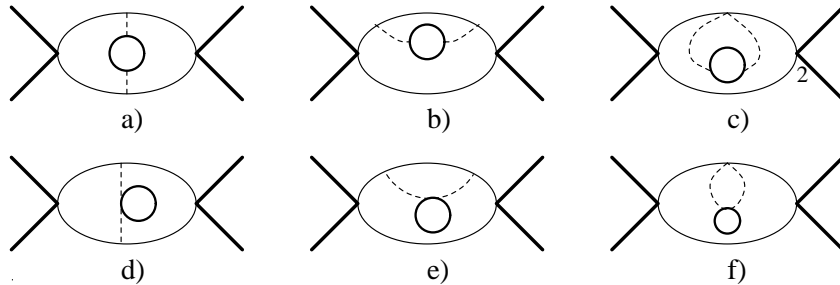


Figure 8: *The generating thermal diagrams involved in an order- e^2 contribution to the photon number spectrum. Dashed lines: photons. Thin lines: ϕ , ϕ^\dagger particles. Bold lines: Φ particles. Half-bold lines: electrons.*

It is easy to see that out of these 6 generating thermal diagrams we get 41 non-vanishing cut diagrams (10 from a); 9 from b); 4 from c); 8 from d); 4 from e) and 6 from f).) The actual electron number spectrum calculations are thus rather long and not extremely rewarding for our unphysical toy model, so we refrain from doing them.

6 Conclusions

In this paper we have formulated a systematic method for studying the heat-bath particle number spectrum using modified cut diagrams. In particular, for the quark-gluon plasma in thermodynamical equilibrium our approach should be useful as an effective alternative to the Landshoff and Taylor [3] approach. The method used in [3] (i.e. to start from first principles) suffers from the lack of a systematic computational approach for higher orders in coupling constants. One of the corner stones of our formalism is the largest-time equation (LTE). We have shown how the zero-temperature LTE can be extended to finite temperature. During the course of this analysis, we have emphasized some important properties of the finite-temperature extension which are worth mentioning. Firstly, many of kinematic rules valid for zero-temperature diagrams can not be directly used in the finite-temperature ones. This is because the emission or absorption of heat-bath particles make it impossible to fix some particular direction to a diagrammatic line. It turns out that one finds more diagrams then one used to have at zero temperature. The most important reductions of the diagrams have been proved. The rather complicated structure of the finite-temperature diagrams brings into play another complication: uncuttable diagrams. It is well known that at zero temperature one can always make only one cut in each cut diagram (this can be viewed as a consequence of the unitarity condition). This is not true however at finite temperature. We have found it as useful to start fully with the LTE analysis which is in terms of type 1 and type 2 vertices. This language allows us

to construct systematically all the cut diagrams. We have refrained from an explicit use of the cuts in finite-temperature diagrams as those are ambiguous and therefore rather obscure the analysis.

The second, rather technical, corner stone is the thermal Dyson-Schwinger equation. We have developed a formalism of the *arrowed* variations acting directly on field operators. This provides an elegant technique for dealing in a practical fashion with expectation values (both thermal and vacuum) whenever functions or functionals of fields admit the decomposition (A.1). The merit of the Dyson-Schwinger equation is that it allows us to rewrite an expectation value of some functional of field in terms of expectation values of less complicated functionals. Some illustrations of this and further thermal functional identities are derived in Appendix A.

When we have studied the heat-bath particle number spectrum, we applied the Dyson-Schwinger equation both to numerator and denominator of corresponding expression. The results were almost the same. The simple modification of one propagator rendered both equal. We could reflect this on a diagrammatical level very easily as the denominator was fully expressible in terms of thermal cut diagrams. Our final rule for the heat-bath particle spectrum is

$$\frac{d\Delta\langle N(\omega)\rangle}{d\omega} = \frac{\langle T^\dagger \mathcal{P} T \rangle_{p_1 p_2, \beta}^M}{\langle T^\dagger \mathcal{P} T \rangle_{p_1 p_2, \beta}}, \quad (6.1)$$

with T being the T -matrix, \mathcal{P} being the projection operator onto final states, p_1, p_2 being the momenta of particles in the initial state, β being the inverse temperature and M being abbreviation for the modified digrams. Modification of the cut diagrams consist of the substitution in turn of each heat-bath particle line by an altered one. This substitution must be done in each cut diagram. Replacement must be only one per modified diagram. Our approach is demonstrated on a simple model where two scalar particles (“pions”) scatter, within a photon-electron heat bath, into a pair of charged particles (“muon” and “antimuon”) and it is shown how to calculate the resulting changes in the number spectra of the photons and electrons.

Acknowledgements

We are indebted to P.V.Landshoff for reading the manuscript and for invaluable discussion. The work is supported in part by Fitzwilliam College scholarship.

A Appendix

A.1 Functional formalism: general background

Eq.(2.18) gives us an alternative definition of the Dyson-Schwinger equation in terms of the “functional derivation” $\frac{\delta}{\delta\psi(x)}$. Let us first show that (2.18) is consistent with Wick’s theorem (2.16)-(2.17). To be specific, let us consider an ensemble of non-interacting

particles in thermodynamical equilibrium. In order to keep the work transparent, we shall suppress all the internal indices. There is no difficulty whatsoever in reintroducing the necessary details. Let us first realize that for any (well behaved) functional the following Taylor's expansion holds ^[17]

$$X[\psi] = \sum_n \int dx_1 \dots \int dx_n \alpha^n(x_1 \dots x_n) \psi(x_1) \dots \psi(x_n), \quad (\text{A.1})$$

The same is true if ψ is an operator instead. In the latter case the $\alpha^n(\dots)$ are not generally symmetric in the x 's **. When Fermi fields are involved, we might, for the sake of compactness, include in the argument of ψ the space-time coordinate, the Dirac index, and a discrete index which distinguishes ψ_α from $\bar{\psi}_\alpha$. In the latter case $\int dx \rightarrow \sum \int dx$, where a summation runs over the discrete indices. With this convention, the expansion (A.1) holds even for the Fermi fields. An extension of (A.1) to the case where different fields are present is natural. Particularly important is the case when ψ is a field in the interaction picture, using Wick's theorem and decomposition (A.1) one can then write

$$\begin{aligned} \langle G[\psi] \psi(x) F[\psi] \rangle_\beta &= \\ &= \sum_{m,n} \left(\int dx \right)^n \left(\int dy \right)^m \alpha^n(x_1 \dots x_n) \beta^m(y_1 \dots y_m) \left\langle \left(\prod_k^n \psi(x_k) \right) \psi(x) \prod_{k'}^m \psi(y_{k'}) \right\rangle_\beta \\ &= \sum_n \left(\int dx \right)^n \alpha^n(x_1 \dots x_n) \sum_l (\pm 1)^{n-l} \langle \psi(x_l) \psi(x) \rangle_\beta \left\langle \prod_{k \neq l}^n \psi(x_k) F[\psi] \right\rangle_\beta \\ &+ \sum_m \left(\int dy \right)^m \beta^m(y_1 \dots y_m) \sum_l (\pm 1)^{l-1} \langle \psi(x) \psi(y_l) \rangle_\beta \left\langle G[\psi] \prod_{k' \neq l}^m \psi(y_{k'}) \right\rangle_\beta. \end{aligned} \quad (\text{A.2})$$

with $(\int dx)^n = \int dx_1 \dots \int dx_n$. The ‘-’ stands for fermions and ‘+’ for bosons. On the other hand, using the formal prescriptions (2.19) and (2.21) for $\frac{\overrightarrow{\delta}}{\delta \psi(x)}$ one can read

$$\begin{aligned} \int dz \langle \psi(x) \psi(z) \rangle_\beta \left\langle G[\psi] \frac{\overrightarrow{\delta} F[\psi]}{\delta \psi(z)} \right\rangle_\beta &= \\ &= \sum_m \left(\int dy \right)^m \beta^m(y_1 \dots y_m) \int dz \langle \psi(x) \psi(z) \rangle_\beta \sum_l^m (\pm 1)^{l-1} \delta(z - y_l) \left\langle G[\psi] \prod_{k' \neq l}^m \psi(y_{k'}) \right\rangle_\beta \\ &= \sum_m \left(\int dy \right)^m \beta^m(y_1 \dots y_m) \sum_l^m (\pm 1)^{l-1} \langle \psi(x) \psi(y_l) \rangle_\beta \left\langle G[\psi] \prod_{k' \neq l}^m \psi(y_{k'}) \right\rangle_\beta. \end{aligned} \quad (\text{A.3})$$

Similar expression holds for $\int dz \langle \psi(x) \psi(z) \rangle_\beta \left\langle \frac{G[\psi] \overleftarrow{\delta}}{\delta \psi(z)} F[\psi] \right\rangle_\beta$. Putting latter two together we get precisely (A.2). This confirms the validity of (2.18). It is easy to persuade oneself that exactly the same sort of arguments leads to

**If $X = X[\psi, \partial\psi]$, the α^n may also contain derivations working on the various fields. In this paper we rule out such a case from our reasonings.

$$\langle \psi(x)F[\psi] \rangle_\beta = \int dz \langle \psi(x)\psi(z) \rangle_\beta \left\langle \frac{\vec{\delta} F[\psi]}{\delta \psi(z)} \right\rangle_\beta \quad (\text{A.4})$$

$$\langle \mathcal{T}(\psi(x)F[\psi]) \rangle_\beta = \int dz \langle \mathcal{T}(\psi(x)\psi(z)) \rangle_\beta \left\langle \mathcal{T} \left(\frac{\vec{\delta} F[\psi]}{\delta \psi(z)} \right) \right\rangle_\beta \quad (\text{A.5})$$

$$\begin{aligned} \langle G[\psi] \mathcal{T}(\psi(x)F[\psi]) \rangle_\beta &= \int dz \langle \mathcal{T}(\psi(x)\psi(z)) \rangle_\beta \left\langle G[\psi] \mathcal{T} \left(\frac{\vec{\delta} F[\psi]}{\delta \psi(z)} \right) \right\rangle_\beta + \\ &+ \int dz \langle \psi(z)\psi(x) \rangle_\beta \left\langle \frac{G[\psi] \overleftarrow{\delta}}{\delta \psi(z)} \mathcal{T}(F[\psi]) \right\rangle_\beta, \end{aligned} \quad (\text{A.6})$$

etc.

with \mathcal{T} being either the chronological or anti-chronological time ordering symbol. At this stage it is important to realize that from the definition of $\frac{\vec{\delta}}{\delta \psi(x)}$ directly follows that $[\frac{\vec{\delta}}{\delta \psi(x)}; \frac{\vec{\delta}}{\delta \psi(y)}]_\mp = 0$ (‘-’ holds for bosons and ‘+’ for fermions). Indeed,

$$\begin{aligned} \frac{\vec{\delta}^2 F[\psi]}{\delta \psi(x) \delta \psi(y)} &= \sum_{n=2} \sum_{i < j} \left(\int dx \right)^{n-2} (\alpha^n(x_1 \dots \overset{x_i}{\downarrow} \overset{x_j}{\downarrow} \dots x_n) \pm \\ &\pm \alpha^n(x_1 \dots \overset{x_i}{\downarrow} \overset{x_j}{\downarrow} \dots x_n)) (\pm 1)^{i+j} \prod_{m \neq i,j}^n \psi(x_m) = \mp \frac{\vec{\delta}^2 F[\psi]}{\delta \psi(y) \delta \psi(x)}. \end{aligned} \quad (\text{A.7})$$

Similarly $[\frac{\overleftarrow{\delta}}{\delta \psi(x)}; \frac{\overleftarrow{\delta}}{\delta \psi(y)}]_\mp = 0$. Analogously we might prove

$$\frac{F[\psi] \overleftarrow{\delta}^2}{\delta \psi(x) \delta \psi(y)} = \frac{\overleftarrow{\delta}^2 F[\psi]}{\delta \psi(x) \delta \psi(y)} \quad (\text{A.8})$$

and

$$\begin{aligned} \frac{\vec{\delta}^2 (F[\psi] G[\psi])}{\delta \psi(x) \delta \psi(y)} &= \frac{F[\psi] \overleftarrow{\delta}^2}{\delta \psi(x) \delta \psi(y)} G[\psi] + (-1)^p \frac{F[\psi] \overleftarrow{\delta}}{\delta \psi(x)} \frac{\vec{\delta} G[\psi]}{\delta \psi(y)} \\ &+ \frac{F[\psi] \overleftarrow{\delta}}{\delta \psi(y)} \frac{\vec{\delta} G[\psi]}{\delta \psi(x)} + F[\psi] \frac{\overleftarrow{\delta}^2 G[\psi]}{\delta \psi(x) \delta \psi(y)}. \end{aligned} \quad (\text{A.9})$$

The “ p ” is 0 for bosons and 1 for fermions. With (2.18) and (A.4) - (A.6) one can easily construct more complicated expectation values. For example, using (2.18) and (A.4) we get

$$\langle \psi(x)\psi(y)F[\psi] \rangle_\beta =$$

$$\begin{aligned}
&= \int \frac{dz_1 dz_2}{2} (\langle \psi(x) \psi(z_1) \rangle_\beta \langle \psi(y) \psi(z_2) \rangle_\beta + (-1)^p \langle \psi(x) \psi(z_2) \rangle_\beta \langle \psi(y) \psi(z_1) \rangle_\beta) \\
&\quad \times \left\langle \frac{\overrightarrow{\delta^2} F[\psi]}{\delta \psi(z_1) \delta \psi(z_2)} \right\rangle_\beta \\
&+ \langle \psi(x) \psi(y) \rangle_\beta \langle F[\psi] \rangle_\beta.
\end{aligned} \tag{A.10}$$

Similarly, using (2.18) and (anti-)commutativity of the arrowed $\frac{\delta}{\delta \psi(x)}$, we get

$$\begin{aligned}
&\langle G[\psi] \psi(x) \psi(y) F[\psi] \rangle_\beta = \\
&= \int \frac{dz_1 dz_2}{2} (\langle \psi(x) \psi(z_1) \rangle_\beta \langle \psi(y) \psi(z_2) \rangle_\beta + (-1)^p \langle \psi(x) \psi(z_2) \rangle_\beta \langle \psi(y) \psi(z_1) \rangle_\beta) \\
&\quad \times \left\langle G[\psi] \frac{\overrightarrow{\delta^2} F[\psi]}{\delta \psi(z_1) \delta \psi(z_2)} \right\rangle_\beta \\
&+ \int \frac{dz_1 dz_2}{2} (\langle \psi(z_1) \psi(x) \rangle_\beta \langle \psi(z_2) \psi(y) \rangle_\beta + (-1)^p \langle \psi(z_2) \psi(x) \rangle_\beta \langle \psi(z_1) \psi(y) \rangle_\beta) \\
&\quad \times \left\langle \frac{G[\psi] \overleftarrow{\delta^2}}{\delta \psi(z_1) \delta \psi(z_2)} F[\psi] \right\rangle_\beta \\
&+ \int dz_1 dz_2 (\langle \psi(z_1) \psi(x) \rangle_\beta \langle \psi(y) \psi(z_2) \rangle_\beta + (-1)^p \langle \psi(x) \psi(z_2) \rangle_\beta \langle \psi(z_1) \psi(y) \rangle_\beta) \\
&\quad \times \left\langle \frac{G[\psi] \overleftarrow{\delta} \overrightarrow{\delta} F[\psi]}{\delta \psi(z_1) \delta \psi(z_2)} \right\rangle_\beta \\
&+ \langle \psi(x) \psi(y) \rangle_\beta \langle G[\psi] F[\psi] \rangle_\beta.
\end{aligned} \tag{A.11}$$

We could proceed further having still higher powers of fields and variations. However, there is a quite interesting generalization in case when we have (anti-)time ordered operators. Let us have $F[\psi] = \mathcal{T}(F[\psi])$, in this case

$$\begin{aligned}
\langle F[\psi] \rangle_\beta &= \sum_n \left(\int dx \right)^n \alpha^n(\dots) \langle \mathcal{T}(\prod_{i=1}^n \psi(x_i)) \rangle_\beta \\
&= \sum_{n=1} \left(\int dx \right)^n \frac{\alpha^n(\dots)}{n} \sum_{i,j} \varepsilon_P \langle \mathcal{T}(\psi(x_i) \psi(x_j)) \rangle_\beta \langle \mathcal{T}(\prod_{m \neq i,j}^n \psi(x_m)) \rangle_\beta + \alpha^0(\dots) \\
&= \int dz_1 dz_2 \langle \mathcal{T}(\psi(z_1) \psi(z_2)) \rangle_\beta \left\langle \frac{\overrightarrow{\delta^2} \overline{F}[\psi]}{\delta \psi(z_2) \delta \psi(z_1)} \right\rangle_\beta + \langle F[0] \rangle_\beta,
\end{aligned} \tag{A.12}$$

where $\overline{F}[\psi]$ differs from $F[\psi]$ in the replacement $\alpha^n(\dots) \rightarrow \frac{\alpha^n(\dots)}{n}$ (n starts from 1 !). In comparison with (A.4)-(A.11), the $\alpha^0(\dots)$ (i.e. the pure $T = 0$ contribution) does matter here. Note that $\alpha^0(\dots)$ generally involves non-heat bath fields with corresponding space-time integrations. Similar extension is true if $F[\psi] = \mathcal{T}_c(F[\psi])$, where \mathcal{T}_c is the time path ordering symbol. In that case

$$\begin{aligned}
\langle F[\psi] \rangle_\beta &= \sum_n \left(\int_C dx \right)^n \alpha^n(\dots) \langle \mathcal{T}_c(\prod_{p=1}^n \psi(x_p)) \rangle_\beta \\
&= \int_C dz_1 dz_2 \langle \mathcal{T}_c(\psi(z_1)\psi(z_2)) \rangle_\beta \left\langle \frac{\vec{\delta}^2 \overline{F}[\psi]}{\delta\psi(z_2)\delta\psi(z_1)} \right\rangle_\beta \\
&+ \langle F[0] \rangle_\beta,
\end{aligned} \tag{A.13}$$

with $\int_C dx = \int_C dt \int_V d\mathbf{x}$ and $\frac{\delta\psi(x)}{\delta\psi(y)} = \delta_C(x-y)$ ^{††}. Wick's theorem for the \mathcal{T}_C -oriented product of fields has an obvious form

$$\langle \mathcal{T}_C(\psi(x_1) \dots \psi(x_{2n})) \rangle_\beta = \sum_{\substack{j \\ j \neq i}} \varepsilon_P \langle \mathcal{T}_C(\psi(x_i)\psi(x_j)) \rangle_\beta \langle \mathcal{T}_C(\prod_{k \neq i,j} \psi(x_k)) \rangle_\beta. \tag{A.14}$$

This can be directly derived from Wick's theorem (2.17), realizing that

$$\mathcal{T}_C(\psi(x_1) \dots \psi(x_m)) = \sum_P \varepsilon_P \theta_C(t_{P_1}, \dots, t_{P_m}) \psi(x_{P_1}) \dots \psi(x_{P_m}), \tag{A.15}$$

where P refers to the permutation of the indices and $\theta_C(t_1, \dots, t_m)$ being a contour step function [26] defined as

$$\theta_C(t_1, \dots, t_m) = \begin{cases} 1 & (t_1, \dots, t_m \text{ are } \mathcal{T}_C\text{-oriented along } C) \\ 0 & (\text{otherwise}) \end{cases} \tag{A.16}$$

Particularly important is the Keldysh-Schwinger path [1, 25, 26], see Fig.9.

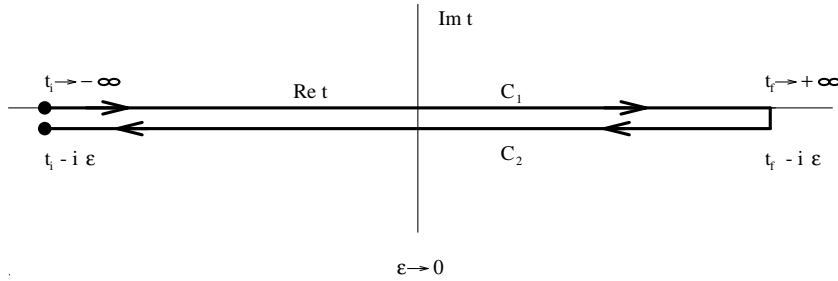


Figure 9: *The Keldysh-Schwinger time path.*

In the latter case

$$\langle F[\psi] \rangle_\beta = \int_{C_1} dz_1 dz_2 \langle \mathcal{T}(\psi(z_1)\psi(z_2)) \rangle_\beta \left\langle \frac{\vec{\delta}^2 \overline{F}[\psi]}{\delta\psi(z_2)\delta\psi(z_1)} \right\rangle_\beta$$

^{††}A contour δ -function $\delta_C(x-y)$ is defined as $\int_C dz \delta_C(z-z') f(z) = f(z')$, see [9, 24].

$$\begin{aligned}
& + \int_{C_2} dz_1 dz_2 \langle \overline{\mathcal{T}}(\psi(z_1)\psi(z_2)) \rangle_\beta \left\langle \frac{\overrightarrow{\delta^2 F}[\psi]}{\delta\psi(z_2)\delta\psi(z_1)} \right\rangle_\beta \\
& + 2 \int_{C_2} dz_1 \int_{C_1} dz_2 \langle \psi(z_1)\psi(z_2) \rangle_\beta \left\langle \frac{\overrightarrow{\delta^2 F}[\psi]}{\delta\psi(z_2)\delta\psi(z_1)} \right\rangle_\beta \\
& + \langle F[0] \rangle_\beta.
\end{aligned} \tag{A.17}$$

Application to the product $G[\psi]F[\psi]$ with $F[\psi] = \mathcal{T}_{C_1}(F[\psi])$ and $G[\psi] = \mathcal{T}_{C_2}(G[\psi])$ is straightforward and reads

$$\begin{aligned}
\langle G[\psi]F[\psi] \rangle_\beta &= \int dz_1 dz_2 \langle \overline{\mathcal{T}}(\psi(z_1)\psi(z_2)) \rangle_\beta \left\langle \frac{\overline{G[\psi]\delta^2}}{\delta\psi(z_2)\delta\psi(z_1)} F[\psi] \right\rangle_\beta \\
&+ \int dz_1 dz_2 \langle \mathcal{T}(\psi(z_1)\psi(z_2)) \rangle_\beta \left\langle \overline{G[\psi] \frac{\overrightarrow{\delta^2 F}[\psi]}{\delta\psi(z_2)\delta\psi(z_1)}} \right\rangle_\beta \\
&+ 2 \int dz_1 dz_2 \langle \psi(z_1)\psi(z_2) \rangle_\beta \left\langle \overline{\frac{G[\psi]\delta}{\delta\psi(z_1)} \frac{\overrightarrow{\delta F}[\psi]}{\delta\psi(z_2)}} \right\rangle_\beta \\
&+ \langle G[0]F[0] \rangle_\beta,
\end{aligned} \tag{A.18}$$

where the overlining indicates that we work with $\frac{\alpha^n(\dots)\beta^m(\dots)}{n+m}$ instead of $\alpha^n(\dots)\beta^m(\dots)$, we have also abbreviated $\int_{C_1} dz$ to $\int dz \int_{C_1} dz$. We should also emphasize that $\frac{\delta\psi(x)}{\delta\psi(y)}$ used in (A.18) is $\delta(x-y)$ rather than $\delta_C(x-y)$.

In Eq.(4.3) it has been used the inverted version of (A.18), namely

$$\begin{aligned}
\langle (G[\psi]F[\psi])' \rangle_\beta &= \int \frac{dz_1 dz_2}{2} \langle \overline{\mathcal{T}}(\psi(z_1)\psi(z_2)) \rangle_\beta \left\langle \frac{G[\psi]\delta^2}{\delta\psi(z_2)\delta\psi(z_1)} F[\psi] \right\rangle_\beta \\
&+ \int \frac{dz_1 dz_2}{2} \langle \mathcal{T}(\psi(z_1)\psi(z_2)) \rangle_\beta \left\langle G[\psi] \frac{\overrightarrow{\delta^2 F}[\psi]}{\delta\psi(z_2)\delta\psi(z_1)} \right\rangle_\beta \\
&+ \int dz_1 dz_2 \langle \psi(z_1)\psi(z_2) \rangle_\beta \left\langle \frac{G[\psi]\delta}{\delta\psi(z_1)} \frac{\overrightarrow{\delta F}[\psi]}{\delta\psi(z_2)} \right\rangle_\beta,
\end{aligned} \tag{A.19}$$

Here $(G[\psi]F[\psi])'$ has the coefficients $\alpha^n(\dots)\beta^m(\dots)\frac{(n+m)}{2}$ instead of $\alpha^n(\dots)\beta^m(\dots)$. Note, that the $\alpha^0(\dots)\beta^0(\dots)$ does not contribute and thus we do not have any pure $T=0$ contributions. Eq.(A.19) has a natural interpretation. Whilst the LHS tells us, that from each thermal diagram (constructed out of $\langle G[\psi]F[\psi] \rangle_\beta$) with $\frac{n+m}{2}$ internal heat-bath particle lines we must take $n+m$ identical copies, the RHS says, that this is virtually because we sum over all possible distributions of one heat-bath particle line inside of the given diagram. The pictorial expression of (A.19) is depicted in Fig.10.

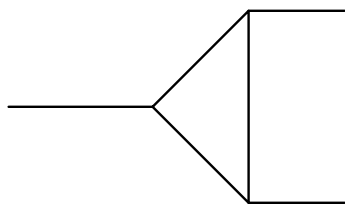
$$\text{Diagram} \times (\text{number of lines}) = \sum_{\substack{i,j \\ i \neq j}} \text{Diagram}_1 + \sum_{\substack{i,j \\ i \neq j}} \text{Diagram}_2 + \sum_{i,j} \text{Diagram}_3$$

Figure 10: *Diagrammatic equivalent of Eq.(A.19). The cut separates areas constructed out of $F[\psi]$ and $G[\psi]$.*

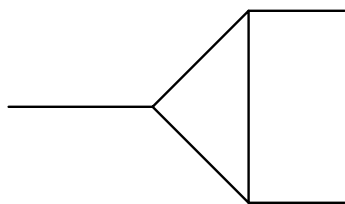
References

- [1] M.LeBellac, Thermal Field Theory (Cambridge University Press, 1996)
- [2] N.P.Landsman and Ch.G.van Weert, Physics Reports 145, Nos.3-4 (1987) 141.
- [3] P.V.Landshoff and J.C.Taylor, Nuclear Physics B 430 (1994) 683-694.
- [4] P.V.Landshoff, Phys Lett. B 386 (1966) 291.
- [5] L.V.Keldysh, Sov.Phys. - JETP 20 (1964), 1018.
- [6] P.van Nieuwenhuizen, Canonical methods in quantized gauge field theories (Teyler's lectures, Leyden University, 1992).
- [7] M.Veltman, Diagrammatica - The Path to Feynman Diagrams (Cambridge University Press, Cambridge, 1994).
- [8] G.'t Hooft and M.Veltman, Diagrammar, CERN Yellow report 73-9.
- [9] R.Mills, Propagators for Many-Particle Systems (Gordon and Breach, New York, 1969).
- [10] T.S.Evans and D.A.Steer, Wick's Theorem at Finite Temperature (hep-ph/9601208).
- [11] A.J.Niemi and G.W.Semenoff, Nuclear Physics B 230 (1984) 181.
- [12] T.S.Evans and A.C.Pearson, Preprint Imperial/TP/93-94/09.
- [13] F.Gelis, hep-ph/9412347
- [14] C.Itzykson and J.B.Zuber, Quantum Field Theory (McGraw-Hill, New York, 1980).
- [15] P.F.Badeque, A.Das and S.Naik, hep-ph/9603325.
- [16] R.L.Kobes and G.W.Semenoff, Nuclear Physics B272 (1986) 329.
- [17] P.Ramond, Field Theory, A Modern Primer (The Benjamin/Cummings Publishing Company, INC, London, 1981).
- [18] M.Jacob and P.V.Landshoff, Phys Lett. B 281 (1992) 114.

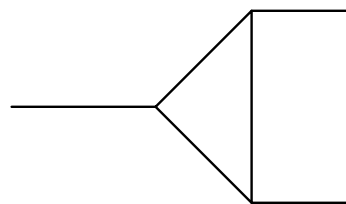
- [19] J.I.Kapusta, Nuclear Physics B 148 (1979) 461
- [20] P.V.Landshoff and A.Rebhan, Nuclear Physics B 410 (1993) 23.
- [21] U.Heinz, K.Kajantie and T.Toimela, Ann.Phys. 176 (1987) 218.
- [22] J.I.Kapusta, Finite-temperature field theory (Cambridge University Press, Cambridge, 1989).
- [23] E.M.Lifshitz and L.P.Pitaevskii, Statistical Physics, part 2 (Pergamon Press, Oxford, 1980).
- [24] A.J.Niemi and G.W.Semenoff, Ann. Phys. 152 (1984) 181.
- [25] J.I.Kapusta and P.V.Landshoff, Nucl.Part.Phys. 15 (1989) 267.
- [26] M.van Eijck, Thermal Field Theory and the Finite-Temperature Renormalization Group (Diploma thesis at the University of Amsterdam, 1995)
- [27] A.L.Fetter and J.D.Walecka, Quantum Theory of Many Particle Systems (New York, McGraw-Hill, 1971).



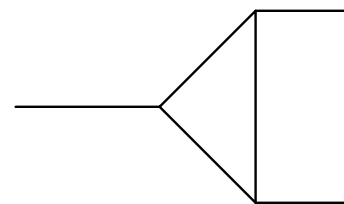
a)



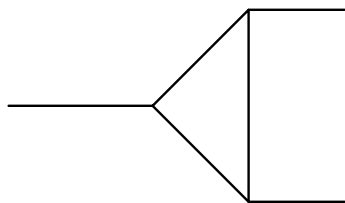
b)



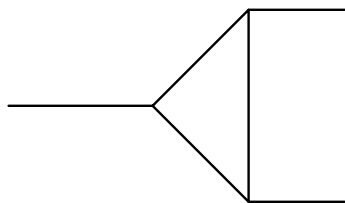
c)



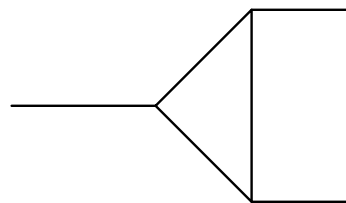
d)



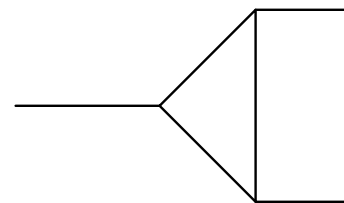
e)



f)



g)



h)

x _____ y

x ○ ————— y

x ○ ————— y

x —————○ y

$$x \quad \text{-----} \quad y \quad = \quad \Delta_{\{F\}}(x-y)$$

$$x \quad \bigcirc \text{-----} \bigcirc \quad y \quad = \quad (\Delta_{\{F\}}(x-y))^{\{*\}}$$

$$x \quad \bigcirc \text{-----} \quad y \quad = \quad \Delta_{\{1\}}(x-y)$$

$$x \quad \text{-----} \bigcirc \quad y \quad = \quad \Delta_{\{2\}}(x-y)$$

$$x \frac{1}{\quad}^1 y \quad \sim \quad i \Delta_F (x-y)$$

$$x \frac{1}{\quad}^2 y \quad \sim \quad i \Delta^- (x-y)$$

$$x \frac{2}{\quad}^1 y \quad \sim \quad i \Delta^+ (x-y)$$

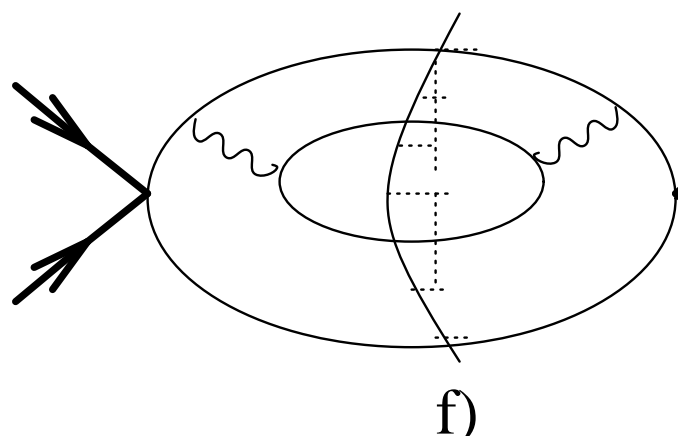
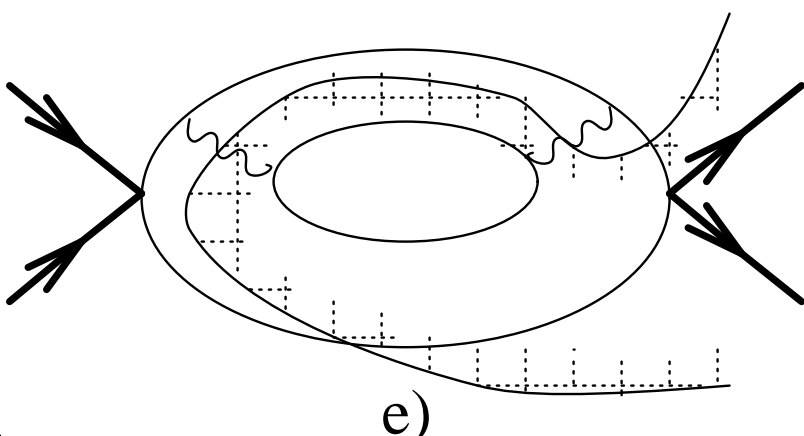
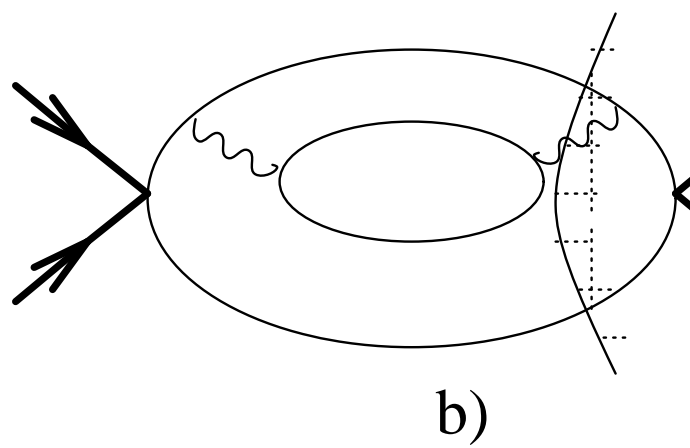
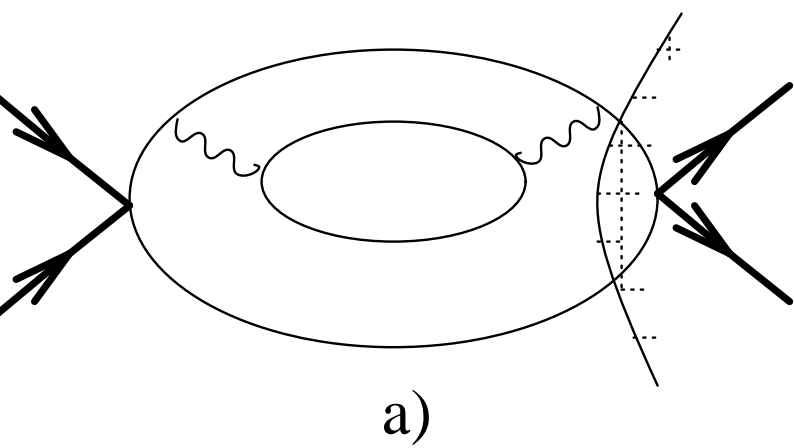
$$x \frac{2}{\quad}^2 y \quad \sim \quad -i \Delta_F^* (x-y)$$

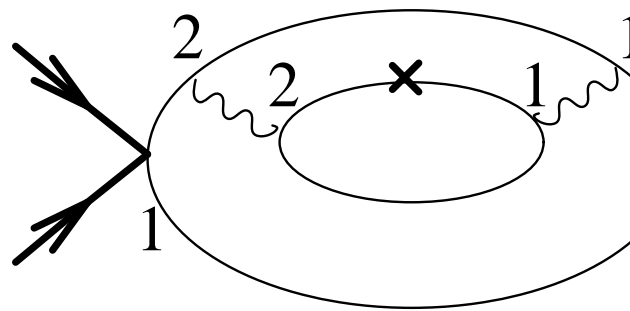
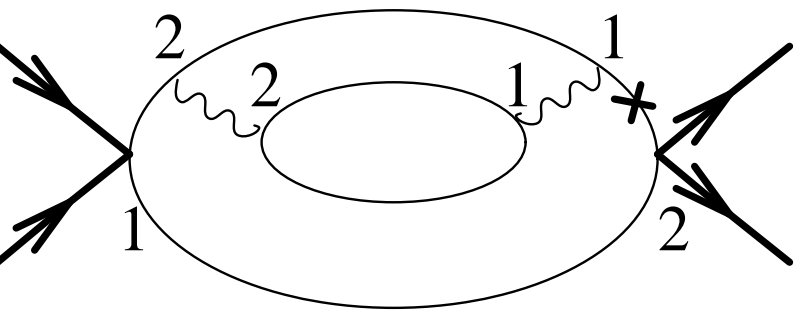
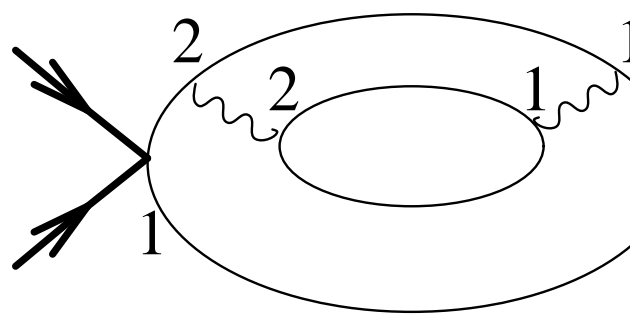
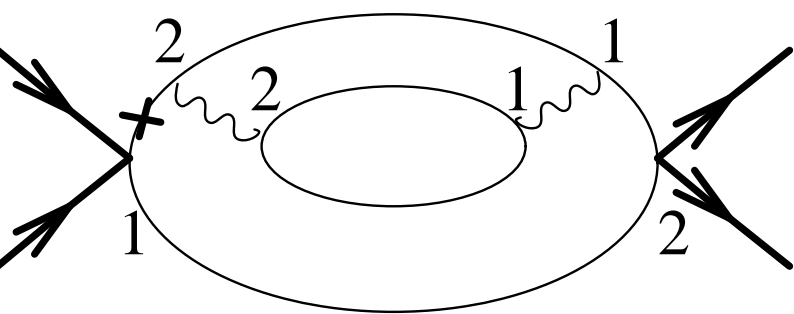
$$x \overset{1}{\rule{1.5cm}{0.4pt}} \overset{1}{y} \quad \sim \quad i \Delta_{\text{F}}(x-y)$$

$$x \overset{1}{\rule{1.5cm}{0.4pt}} \overset{2}{y} \quad \sim \quad i \Delta^{-}(x-y)$$

$$x \overset{2}{\rule{1.5cm}{0.4pt}} \overset{1}{y} \quad \sim \quad i \Delta^{+}(x-y)$$

$$x \overset{2}{\rule{1.5cm}{0.4pt}} \overset{2}{y} \quad \sim \quad -i \Delta_{\text{F}}^{*}(x-y)$$



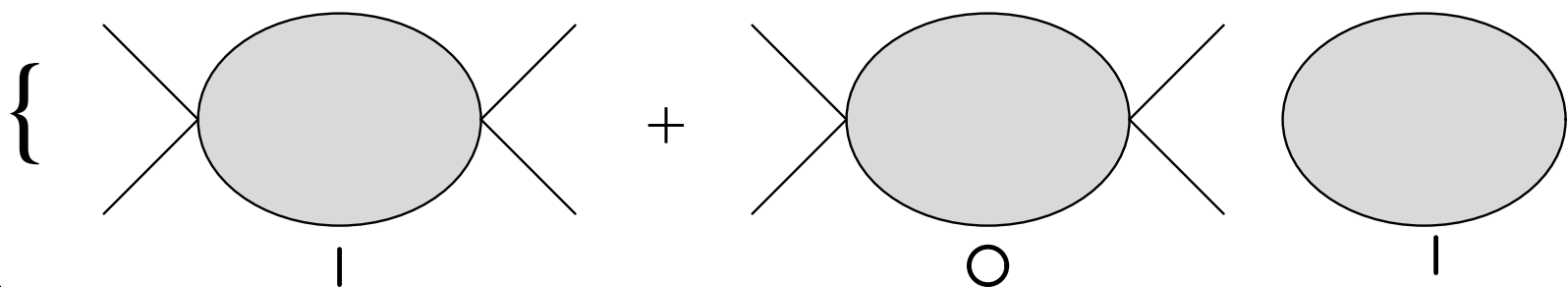


$$\text{x} \overset{1}{\text{---}} \times \overset{1}{\text{---}} \text{y} \quad \sim \quad i\tilde{\text{D}}(\text{x}, \text{y}; \dots)$$

$$\text{x} \overset{1}{\text{---}} \times \overset{2}{\text{---}} \text{y} \quad \sim \quad i\tilde{\Delta}(\text{y}, \text{x}; \dots)$$

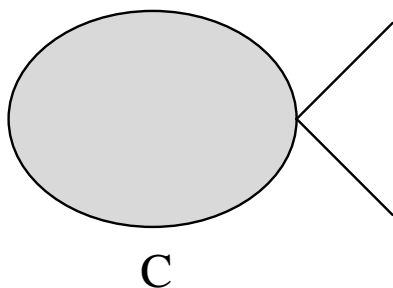
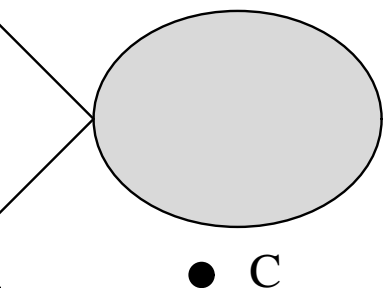
$$\text{x} \overset{2}{\text{---}} \times \overset{1}{\text{---}} \text{y} \quad \sim \quad i\tilde{\Delta}(\text{x}, \text{y}; \dots)$$

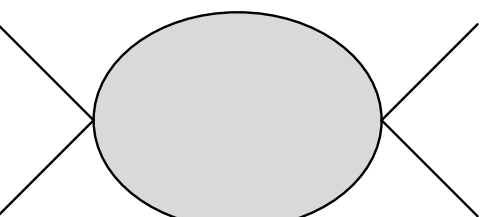
$$\text{x} \overset{2}{\text{---}} \times \overset{2}{\text{---}} \text{y} \quad \sim \quad -i\tilde{\text{D}}^*(\text{x}, \text{y}; \dots)$$



$$\begin{array}{c}
 \diagup \quad \text{c} \quad \diagdown \\
 \text{c}
 \end{array}
 \left(1 + \begin{array}{c} \text{d} \end{array} \right) \begin{array}{c} \bullet \\ \text{c} \end{array} ,$$

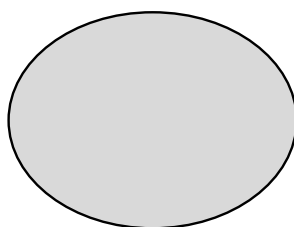
a)





• X C

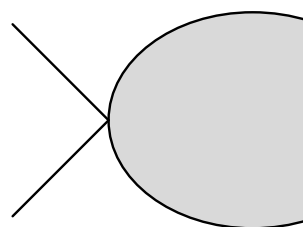
(1 +



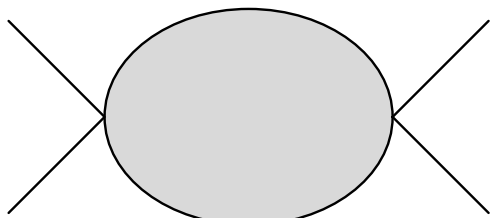
d

)

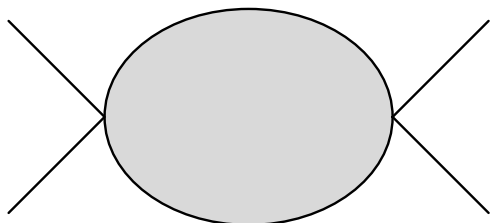
+



• C



● × d



● d

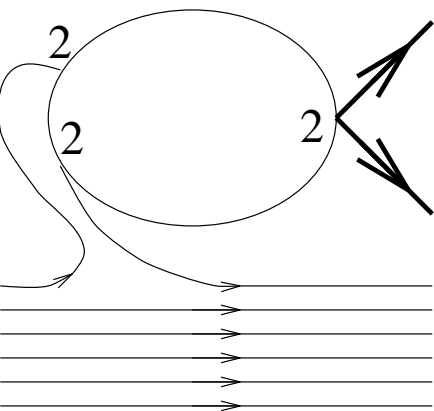
$$x \overset{1}{\text{---}} \times \overset{1}{\text{---}} y \quad \approx \quad \text{fluctuations}$$

$$x \overset{1}{\text{---}} \times \overset{2}{\text{---}} y \quad \approx \quad \text{fluctuations} + \text{emissions} + \text{absorbtions}$$

$$x \overset{2}{\text{---}} \times \overset{2}{\text{---}} y \quad \approx \quad \text{fluctuations}$$

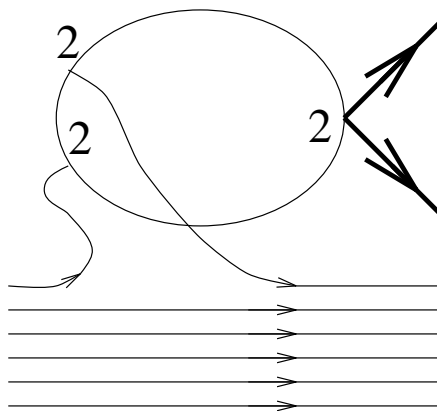
$$\begin{aligned}
 & \left(\begin{array}{c} \text{Diagram 1} \end{array} \right) + \left(\begin{array}{c} \text{Diagram 2} \end{array} \right) = 0
 \end{aligned}$$

$T=0$



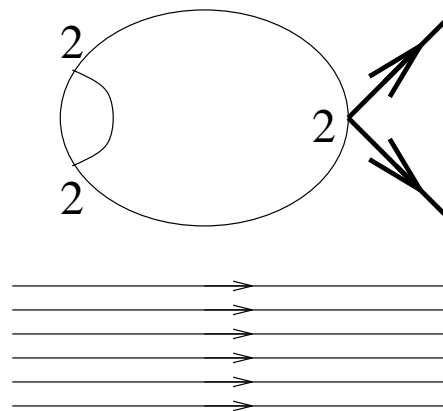
a)

+

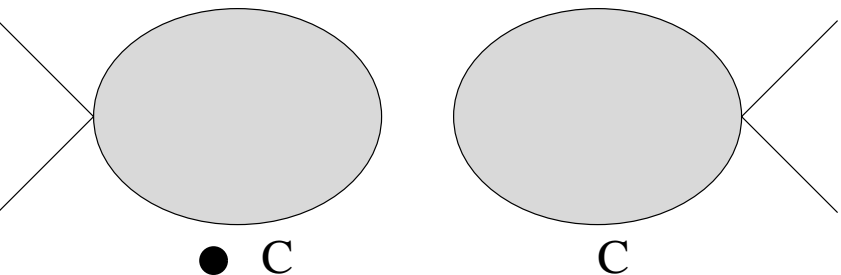


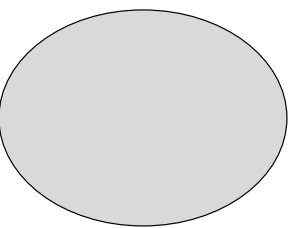
b)

+



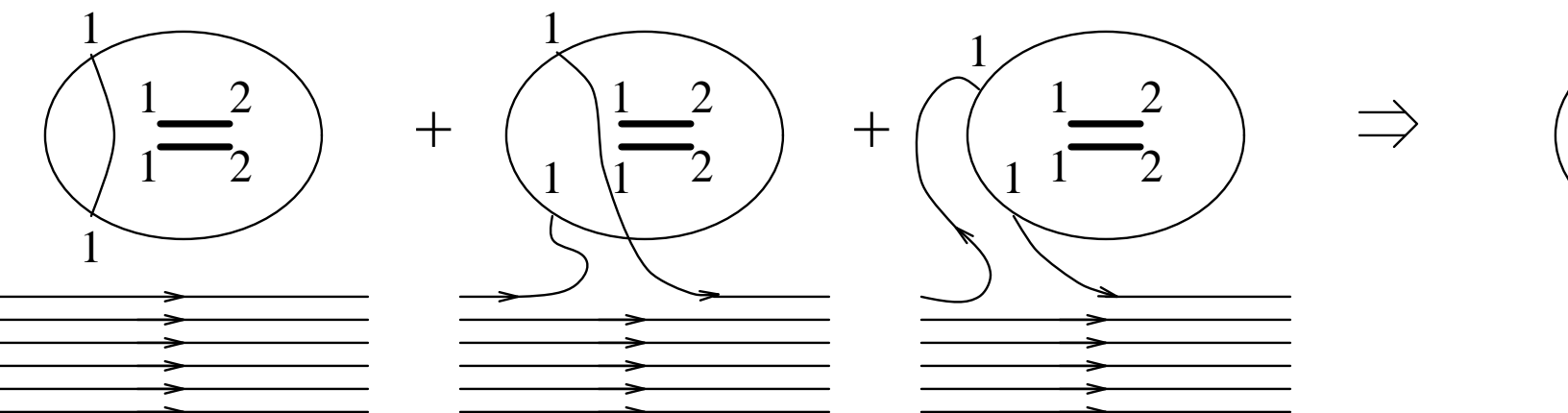
c)



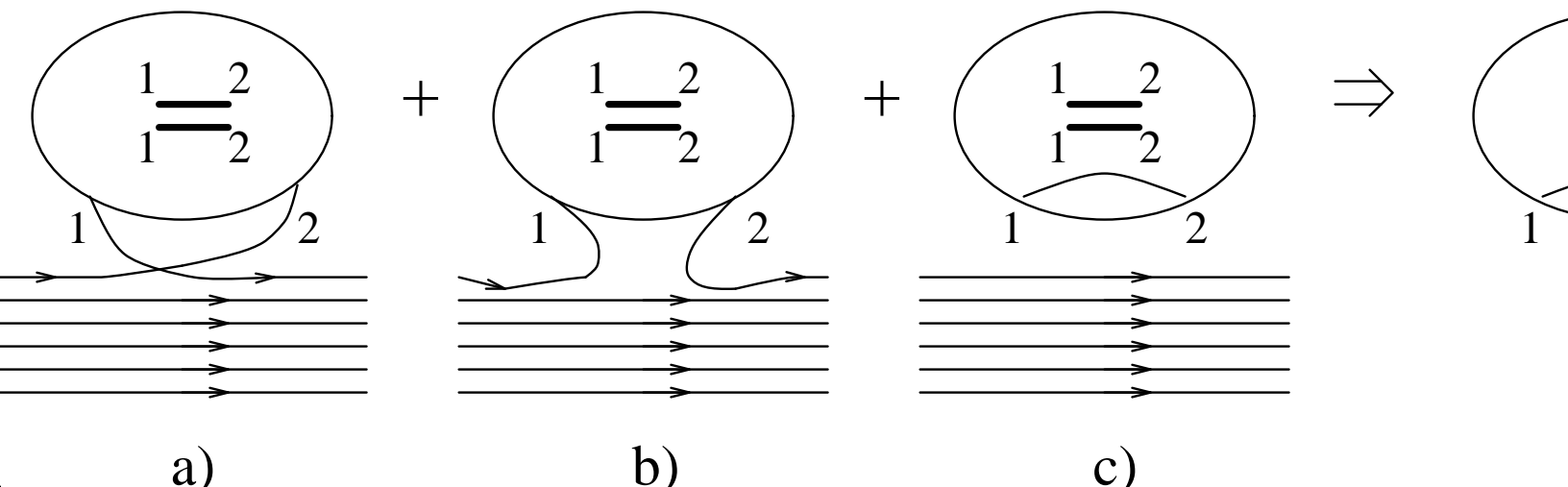


C

T=0



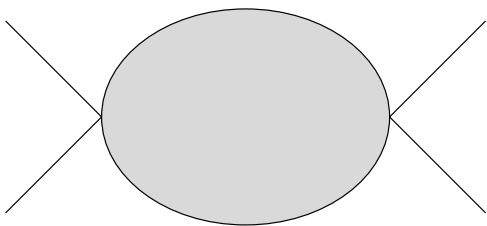
$T=0$



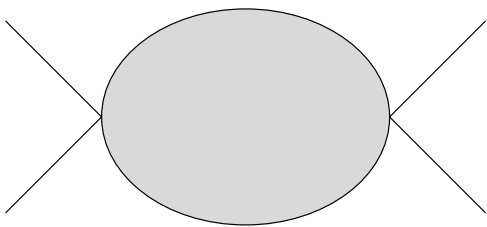
$$(1 + \text{d}) \{ \text{X} \bullet \text{C} + \text{C} \bullet \}$$

$$+ \text{X} \text{C} + \bullet \text{C} + \text{C} \text{X}$$

$$+ \text{C} \text{X} + \bullet \text{C} + \text{X} \text{C} \}$$



● × d



● d

$$(1 + \text{O}) \{ \text{MI} + \text{I} +$$

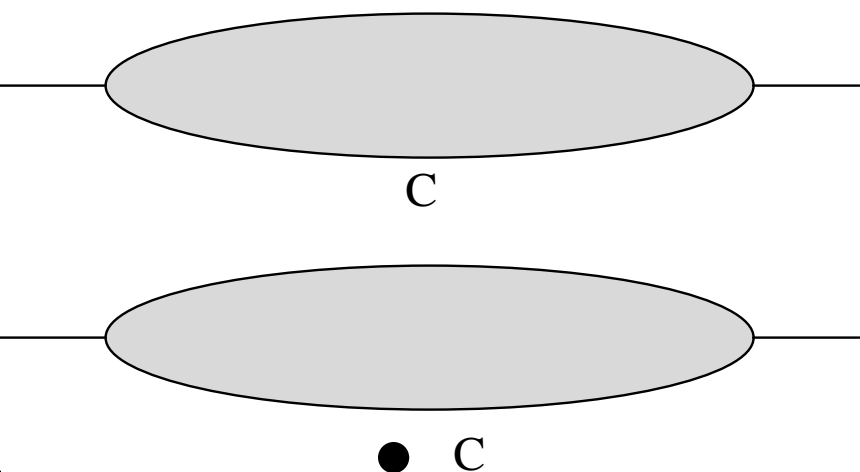
A diagrammatic equation. On the left, a large gray oval labeled 'O' is preceded by a plus sign and enclosed in parentheses. This is followed by a large curly brace. Inside the brace, there are three terms: a gray oval labeled 'MI' with two diagonal lines crossing at its center, a gray oval labeled 'I', and a plus sign followed by another gray oval.

$$+ \text{MO} + \text{I} + \text{O}$$

A diagrammatic equation. It starts with a plus sign followed by a gray oval labeled 'MO' with two diagonal lines crossing at its center. This is followed by a plus sign, a gray oval labeled 'I', another plus sign, and finally a gray oval labeled 'O' with two diagonal lines crossing at its center.

$$+ \text{O} + \text{I} + \text{MO} \}$$

A diagrammatic equation. It starts with a plus sign followed by a gray oval labeled 'O' with two diagonal lines crossing at its center. This is followed by a plus sign, a gray oval labeled 'I', another plus sign, a gray oval labeled 'MO', and finally a large closing curly brace.

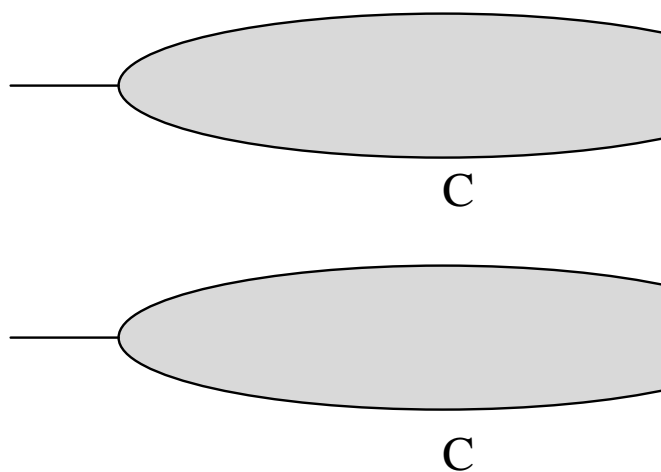


C



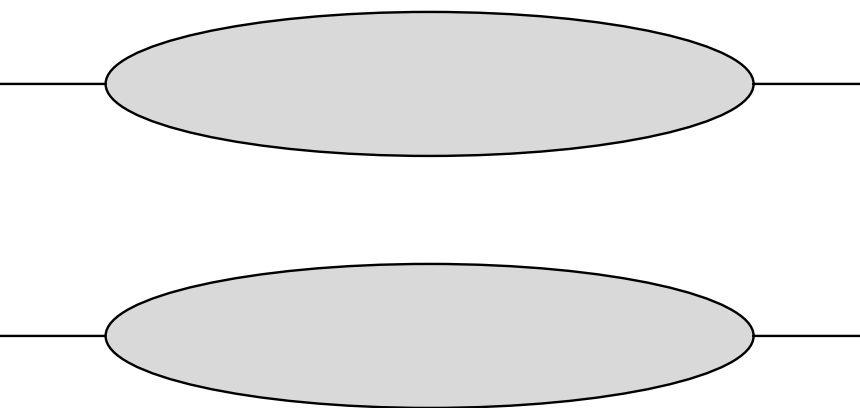
C

;



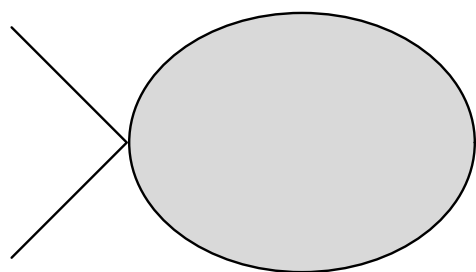
C

C



a)

;



o

b)